nature protocols

REVIEW ARTICLE

https://doi.org/10.1038/s41596-020-0357-x

Check for updates

Tutorial: design and fabrication of nanoparticle-based lateral-flow immunoassays

Claudio Parolo[1,5], Amadeo Sena-Torralba[1,5], José Francisco Bergua[1], Enric Calucho[1], Celia Fuentes-Chust[1], Liming Hu[1], Lourdes Rivas[1], Ruslan Álvarez-Diduk[1], Emily P. Nguyen[1], Stefano Cinti[2], Daniel Quesada-González[3] and Arben Merkoçi[1,4]✉

Lateral-flow assays (LFAs) are quick, simple and cheap assays to analyze various samples at the point of care or in the field, making them one of the most widespread biosensors currently available. They have been successfully employed for the detection of a myriad of different targets (ranging from atoms up to whole cells) in all type of samples (including water, blood, foodstuff and environmental samples). Their operation relies on the capillary flow of the sample throughout a series of sequential pads, each with different functionalities aiming to generate a signal to indicate the absence/presence (and, in some cases, the concentration) of the analyte of interest. To have a user-friendly operation, their development requires the optimization of multiple, interconnected parameters that may overwhelm new developers. In this tutorial, we provide the readers with: (i) the basic knowledge to understand the principles governing an LFA and to take informed decisions during lateral flow strip design and fabrication, (ii) a roadmap for optimal LFA development independent of the specific application, (iii) a step-by-step example procedure for the assembly and operation of an LF strip for the detection of human IgG and (iv) an extensive troubleshooting section addressing the most frequent issues in designing, assembling and using LFAs. By changing only the receptors, the provided example procedure can easily be adapted for cost-efficient detection of a broad variety of targets.

The simplicity and low cost of lateral-flow assays (LFAs) have made them one of the most used point-of-care (PoC) sensors[1,2] in various disciplines ranging from diagnostics[3–6] to environmental[7–9] and safety[10–14] analysis. Their success lies in their general design that has remained almost unchanged since their first use as pregnancy tests in 1970s[15]. Although all LFAs simply rely on capillary forces to move the sample along a test strip to generate a measurable signal, their fabrication is far from being straightforward[16]. In fact, to provide the end user with an easy-to-use device, developers must consider and evaluate multiple parameters, some even simultaneously, for optimal performance or market readiness[17]. For a new researcher or developer, this task may prove to be quite daunting. Fortunately, as it is a relatively 'old' and well-known technology, there are several resources online that discuss the general principles of LFAs, and even several guides are provided by both public and private entities[16,18–26]. In addition, searching for 'lateral flow assay' in Scopus generates over 7,700 documents, with many of them describing the development of a new LFA for specific applications. Although the design and optimization of tailored LFAs remain challenging, the target-specific nature of the assay makes it impossible to write a generalizable LFA protocol that works for all applications. Therefore, instead, in this tutorial, we have collected the knowledge to provide a general roadmap that can be used by developers to design, optimize and fabricate an LFA for their specific application(s).

General principles and components of LFAs

From a user perspective, operation of a well-designed LFA is strikingly simple: the assay is executed by adding the sample onto the lateral-flow strip (LF strip), and after a short incubation time, the positive or negative outcome of the test is revealed by the appearance of a line. Having a more detailed look (Fig. 1) at what happens to the sample after its application (assuming for a standard immune sandwich assay, although other formats are also possible; Box 1), we can see that it first encounters the sample pad, which ensures that the characteristics of the sample match those required for optimal detection (pH, ionic strength, viscosity, purity and concentration of blocking agents). Next, the sample reaches the conjugate pad, which releases the labeled detection bioreceptor (e.g., an antibody, often conjugated to a nanoparticle for detection) upon wetting and allows for a first analyte-bioreceptor interaction. The sample then travels through the membrane (also called detection pad). In most LFAs, there are at least two lines on the membrane: (i) the test line, where a capture bioreceptor binds

[1]Nanobioelectronics & Biosensors Group, Institut Català de Nanociència i Nanotecnologia (ICN2), Campus UAB, Barcelona, Spain. [2]Department of Pharmacy, University of Naples "Federico II", Naples, Italy. [3]Paperdrop Diagnostics, Eureka Building, Campus UAB, Barcelona, Spain. [4]ICREA, Institució Catalana de Recerca i Estudis Avançats, Barcelona, Spain. [5]These authors contributed equally: Claudio Parolo, Amadeo Sena-Torralba.
✉e-mail: arben.merkoci@icn2.cat

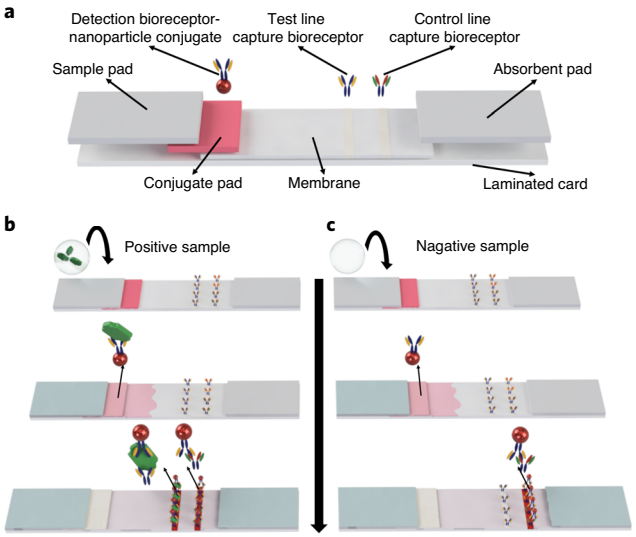

Fig. 1 | Schematic of the main components and operation of a typical LFA. a, An LF strip is made of four main parts: the sample pad, the conjugate pad, the membrane and the absorbent pad. They are mounted on a laminated card. The membrane binds to the capture bioreceptors that form the test and control lines. Panels **b** and **c** show the operation of an LFA based on immunosandwich recognition. **b**, The presence of the target analyte in the sample results in the accumulation of nanoparticles on the test and control lines, making the classical two red lines appear. **c**, In the absence of the target analyte, the nanoparticles accumulate only on the control line, giving a single colored line output.

the labeled analyte, generating a line that indicates the presence or absence of the analyte (most commonly visualized either by the naked eye or by an optical reader); and (ii) the control line, which ensures the correct operation of the LFA (by selective capture of the labeled bioreceptor). Finally, the sample reaches the absorbent pad, which provides enough bed volume for the complete flow of the sample.

Overview of the tutorial

The design of the LF strip strongly depends on the type of sample and the target molecule to be detected (Box 1). Therefore, we start this tutorial by a discussion of the types of samples that can be analyzed and the different challenges this raises. Next, we discuss how to select and characterize appropriate bioreceptors and how to choose the optimal type of nanoparticles for detection. Following this, we have a detailed look at the four main physical components of the LF strip: sample pad, conjugate pad, membrane and absorbent pad. We examine in detail the effects that each component has on the LFA and discuss the key characteristics developers should consider when choosing the most suitable materials and reagents for a specific target of interest. In addition, we provide a detailed step-by-step example procedure for the assembly and operation of an LF strip for detecting human IgG (Box 2).

Types of samples and target analytes

As aforementioned, LFAs are used in various applications with samples that present extremely different composition and characteristics (Table 1)[27]. For example, clinical samples can be whole blood[28,29], plasma[30,31], serum[32–34], sweat[35,36], urine[37,38], stool[39,40], saliva[41,42], cerebrospinal fluid[43,44] and nasal swabs[45,46], while food matrices could be juices[47,48], cereals[49,50], meat[51,52], vegetables[53] and environmental (mostly water and soil) samples[54–57]. Although the sample pad provides a means to control the properties of the sample solution (see the following section), some complex matrices may require pretreatment before an aliquot can be added onto the LF strip[58]. For instance, the most obvious is the requirement for homogeneity of ground solid samples in specific buffers to allow for an even and steady flow through the LFA. When analyzing solid food matrices, large volumes of samples are required for homogenization of unevenly distributed toxic/pathogenic contaminants[59]. In the case of whole blood, its dark red color and viscosity present challenges and various limitations for LFAs. Ideally, the separation of blood cells using external filtration units[60] or by using an integrated special filtration membrane[61,62] on the sample pad is recommended. However, the additional use of external filters may complicate the system for the end user, and sufficient purification is not always achieved. It is also possible to lyse the blood cells before adding the blood sample to the LF strip. However, this should be avoided (unless the target is within the cell) to prevent the release of other proteins and nucleic acids that can interfere with the specificity and sensitivity of the LFA.

Besides making the sample suitable for running in an LFA, developers must also develop a simple yet standardized specimen-collection protocol. To achieve reliable analytical results from different users, it is paramount that the sample-collection procedures are consistent, in particular for LFAs requiring a quantitative reading. For example, LFAs for urinary tests often include a sterile cup to minimize contamination during specimen collection or porous plastic wicks to control the volume of sample and the flow speed. For stool samples, a small spatula is generally included for the uptake of a precise amount of sample and for its immersion in a provided homogenization solution. Nasal, saliva, skin and vaginal samples often provide surface contaminant controls and typically require the use of a cotton swab to capture molecules and particles from inner tissues and surfaces. The swab is then immersed into a provided solution to suspend and pre-treat the sample before its application to the lateral-flow strip. In some special cases, like LFAs for whole blood samples, running and/or washing buffers are used. Their function is to guarantee the flow of the analyte along the LF strip that may be hindered by the viscosity or the insufficient amount of sample.

Bioreceptor selection

For a bioreceptor (typically proteins, antibodies or DNA) to be effective in an LFA, it has to have three main characteristics: (i) it has to be stable, (ii) it needs fast association kinetics and (iii) it should have a strong binding affinity for the target molecule. The stability of the bioreceptor means that it has to keep its structure and functionality in various environments (different temperatures, humidity percentages and pressures)[63], and, above all, it has to maintain its function after a cycle of drying

Box 1 | Types of LFAs

LFAs generally use one of the following two main sensing strategies: competitive or sandwich (non-competitive) assays. Their successful use in LFAs requires the developer to consider important factors during the sensor design, fabrication and optimization.

Competitive assays. There are two main types of competitive formats. In the first type, the target in the sample and a labeled target (alternatively, a molecule with less affinity for the bioreceptor than the target itself) in the conjugate pad compete for the test-line capture bioreceptor[9,213]. In the second type, the target in the sample and the target on the test line (which would act as the test-line capture bioreceptor) compete for the labeled bioreceptor[57,214,215]. A key characteristic of competitive assays is that a higher target concentration results in a lower signal. Competitive assays are generally used for small target molecules (<1 kDa) that cannot be efficiently recognized by more than one bioreceptor (such as drugs and toxins), but they could also be adapted for big analytes. Since competitive assays are not affected by the hook effect[205] (the detection and capture bioreceptors have all their binding sites occupied by single targets, preventing the sandwich formation; this would show a low signal, which may be misinterpreted as absence or a low target concentration), they are particularly useful for the detection of targets with extremely high concentrations. It is important for the developer of a competitive assay to verify that the bioreceptor can recognize the competitor molecule even after it is labeled or adsorbed on the membrane (the use of a spacer to anchor the competitor to the membrane or label may expose it and favor its recognition by the bioreceptor). During the optimization of competitive assays, the concentrations of the detection bioreceptor and test-line capture bioreceptor (generally between 1 and 0.1 mg/ml) are carefully adjusted to not oversaturate the signal in the absence of target, which would produce a low-sensitivity LFA.

Sandwich (non-competitive) assays. A sandwich (non-competitive) assay is probably the most-used strategy for the detection of mid- and big-size analytes (>1 kDa), such as proteins, antibodies, bacteria and cells, in LFAs. It functions by capturing the target molecule between the detection bioreceptor and the test-line capture bioreceptor, producing a signal that increases proportionally with the amount of target in the sample[34,216,217]. One key aspect for the development of this type of assay is the requirement of two bioreceptors that bind different portions of the target. For example, two different monoclonal antibodies or a labeled monoclonal antibody and a capture polyclonal antibody are the most secure ways to ensure the sandwich formation. In the case of particularly big targets, such as bacteria or cells, where the same antigen is repeated many times in the same target, the use of the same antibody (better if polyclonal) would also be a feasible option. As mentioned in the previous paragraph, sandwich assays are subjected to possible hook effects in the case of extremely high target concentrations[205], and they are more prone to false-positive results than competitive assays. For their optimization, higher concentrations of test-line capture bioreceptors are generally recommended (>1 mg/ml) to maximize the chances for the sandwich formation.

and rewetting. In regards to this, fast target analyte binding kinetics are essential, as there are practically no incubation steps on the LFA, and the bioreceptors have to bind to the target within seconds. These two are important characteristics to be considered when selecting suitable antibodies as bioreceptors. In fact, most commercial antibodies are characterized with techniques such as ELISA and western blot. However, these techniques include long incubation steps, typically on the order of hours, and thus antibodies that work for ELISA and western blot may not work for LFA. Finally, the binding between the bioreceptor and the target must be strong to obtain a stable signal. In practice, most of the labeled target will pass through the LFA strip and travel to the detection zone in a matter of seconds. Meanwhile, the flow still continues for minutes and acts as an internal washing step. If the target-to-bioreceptor binding is weak, the signal will decrease over time once the concentration of the labeled analyte in solution decreases.

The choice of the proper bioreceptor is probably the most important step toward achieving the required analytical sensitivity and specificity in an LFA. This is particularly challenging for the detection of protein targets, given the large variety of possible bioreceptors (Table 2). Ideally, during the initial phases of an LFA development, several bioreceptors should be screened using a combinatorial approach where each bioreceptor is tested both in the test line and conjugated to the label nanoparticle. Depending on the resources and facilities available, the use of standard techniques (such as ELISA[64], surface plasmon resonance (SPR)[65], biolayer interferometry (BLI)[66] and isothermal titration calorimetry (ITC)[67])[68] could speed up the screening of multiple bioreceptors. For example, ELISA can be used to evaluate dozens of antibody/antigen combinations to find those producing the most sensitive result in a relatively short amount of time. In this respect, the developer could minimize the duration of the incubation steps to eliminate the bioreceptors with slow binding kinetics. Moreover, SPR, BLI and ITC can provide useful information about the association and dissociation binding kinetics, although they are more expensive techniques than ELISAs. Indeed, these techniques can help to identify and short-list the most promising bioreceptors. However, as the kinetics can be different for binding in porous media, they must be ultimately tested in a real LFA to choose those that will be used in the final assay[69].

Capture bioreceptors versus detection bioreceptors

To avoid confusion, in this article, we refer to the bioreceptors conjugated to the nanoparticles as 'detection bioreceptors' and to the bioreceptors on the membrane as 'capture bioreceptors', which are further divided into 'test-line capture bioreceptors' and 'control-line capture bioreceptors'.

Although it is important to test different combinations of detection and capture bioreceptors (ideally, previously short-listed using standard techniques), from a theoretical perspective, the latter should have a faster binding kinetic. The reason for this is that the interaction of capture bioreceptors with the analyte is limited to the instants during which the flow passes on the test line area, while the detection bioreceptors have slightly more time to bind to the analyte during the flow from the conjugate pad to the test line[17]. Another aspect to consider for the development of a sandwich assay is that the detection bioreceptor should not interfere with the binding of the test-line capture bioreceptor to the target. For example, during the testing of a sandwich assay using a monoclonal antibody and a polyclonal antibody, the monoclonal antibody should be the detection bioreceptor (it binds to just one epitope of the analyte), while the polyclonal antibody should be the test-line capture bioreceptor (the binding to multiple epitopes

Table 1 | Considerations on pH, collection and treatment of different types of samples for their use in LFAs

Sample	pH	Collection	Sample treatment	Reference
Urine	4.5–7.2	Can be directly applied in some LFAs Otherwise use of sterile containers Some patients might not be able to urinate due to a pre-existing condition, requiring catheter extraction	Sample pad buffer should aim at equalizing the pH of different samples Possible dilution or centrifugation	37,38
Blood	7.35–7.45	Fingerprick Venous puncture	If directly applied, a second running buffer is required Use of extra stacking pad for sample filtration	28,29
Plasma	pH 7.35–7.45	Requires the separation of cells from non-clotted blood, generally by centrifugation Special filters can separate plasma from blood without centrifugation, making the ideal approach for LFAs[200]	A running/washing buffer is generally recommended upon sample addition It may require additional filtration before application to the LFA	30,31
Serum	pH 7.35–7.45	Requires separation of the liquid portion from clotted blood, generally by centrifugation	A running/washing buffer is generally recommended upon sample addition It may require additional filtration before application to the LFA	32,33
Sweat	3.5–8.5	The absorbent pad of an LFA is wiped across the skin An absorbent patch is stuck to the skin for several days (e.g., PharmCheck patches)	Use of a running buffer to either extract the sample from the patch or make it run through the sample pad; the sample pad buffer should aim at equalizing the pH of different samples	35,36
Mucus	5.5–8.3	Nasal swabs (including universal transport medium)	Use of a running buffer to extract the sample from the swab The buffer may contain mucins, surfactants and high salt concentrations for viscosity reduction	45,46
Saliva	6.75–7.25	Collection in swabs or tubes Unstimulated: pooling saliva in the mouth and deposited into a specimen tube; it may involve food or drink contamination, higher viscosities and air bubbles Time of collection should be registered for correction of saliva flow rates	Running/extraction buffer may contain mucins, surfactants and high salt concentrations for viscosity reduction Centrifugation and application of the supernatant Stimulated: by chewing gum, by sucking on a lozenge or by swab-like collection devices; it may involve changes in pH, contamination and sample dilution Special salt pad made of glass fiber with highly concentrated salt, placed in the middle of sample pad	41,42,201
Cerebrospinal fluid	7.2–7.4	Lumbar puncture performed by a professional Collection in a sterile container	Directly onto the strip and addition of running buffer Addition of diluent in the container and then application onto the strip	43,44
Stool	6–7.2	Collection in a sterile container, followed by sampling with a dedicated spatula	Homogenization of the sample contained on the spatula in running/extraction buffer; usually with Tween20 for sample disruption	39,40
Water	6.5–8.5	Can be directly applied Some low-concentrated analytes might require concentration of the sample Dirty water may require special filtration	Vacuum pumps and syringes might be used for the sample beforeconcentration	54–57
Solid food	N/A	Uptake of small amount in sterile bags Very different matrices may require different treatments	Generally, homogenization, filtration and dilution Might require extra filtration capabilities Use of running/extraction buffers	49–52,202
Liquid food	N/A	Can be directly applied Uptake of an aliquot in sterile containers	Might require extra filtration capabilities	47,48,102,203

Table 2 | Common bioreceptors used in LFAs for the detection of protein targets

Bioreceptor	Advantages	Disadvantages	Considerations
Polyclonal antibodies	Cost-effective Fast production Multiple binding sites	Low specificity Cross-reactivity Variability between different batches	Affinity purification of the serum is required to minimize cross-reactivity
Monoclonal antibodies	High specificity Low batch-to-batch variability	Expensive Long development process	For immune-sandwich assays, antibodies binding to different epitopes must be chosen, unless the target presents multiple repeated antigens/epitopes (e.g., a membrane protein on the surface of a cell)
Fragments	Less nonspecific binding Once the sequence is known, they are generally cheaper and easier to produce than full-size antibodies Low batch-to-batch variability Ability to increase the number of bioreceptors per probe	Less stable than full-length antibodies since they lack an Fc region	Antibody against IgG Fc region cannot be used in control line. BSA should not be used as a blocking agent, given its higher molecular weight (66 kDa) compared to the fragments (<50 kDa). The possibility of producing some of them as recombinant protein in *E. coli* makes their synthesis easier and cheaper than the immunization of full-length antibodies or using human cell lines
Nanobodies	Less nonspecific binding Once the sequence is known, they are generally cheaper and easier to produce than full-size antibodies Low batch-to-batch variability Ability to increase the number of bioreceptors per probe	Production is limited to *Camelidae* and shark species	BSA should not be used as a blocking agent, given its higher molecular weight (66 kDa) compared to nanobodies (15 kDa)
Aptamers[204]	Cheaper than antibodies Ability to recognize any type of target analyte High stability High batch-to-batch reproducibility	Their binding activity is highly dependent on the ionic strength of the buffer and the presence of interfering molecules in the buffer (i.e., certain cations)	It is recommended to perform a denaturation and refolding step before fabricating the LFA

maximizes the chances of the sandwich formation)[70]. The conjugation/immobilization chemistries, stability and cost should also be considered for each assay development. For example, a bioreceptor may not be compatible with the chosen nanoparticle (i.e., the absence of functional groups for its conjugation), thus forcing the developer to use it as capture bioreceptor. Or, the immobilization of the bioreceptor on the membrane may lead to the unfolding of its structure and the loss of its functionality, while it may be compatible with the nanoparticle surface. Alternatively, the amount of bioreceptor needed for conjugation to the nanoparticle may be considerably higher than the amount needed for its immobilization on the test line, so it may behoove the researchers to use the cheaper bioreceptor as the detection bioreceptor[17].

The characteristics for the control-line capture bioreceptors are less stringent, since they have to bind either the detection bioreceptor or other molecules on the nanoparticle surface. In the case of using an antibody as the detection bioreceptor, the control-line capture bioreceptor could be a secondary polyclonal antibody. Instead, if the detection bioreceptor is a nucleic acid, the control-line capture bioreceptor could be its complementary sequence. Other options such as biotin/streptavidin, BSA/anti-BSA antibodies and similar can also be employed for the generation of the control line.

Selecting nanoparticles for detection

In recent years, the development of new nanomaterials has broadened the type of labels available for LFA, although mostly gold nanoparticles and latex beads are used in mass-manufactured tests (Fig. 2)[71–76]. Here, we describe what we think are the most relevant nanomaterials in regards to their type of readout (also see Table 3 for a summary of the advantages and disadvantages of the different nanoparticles).

Naked-eye detection

The use of particles that allow for naked-eye detection in LFAs is particularly beneficial for qualitative applications or those that aim for cost effectiveness (i.e., not requiring the use of external readers). Nonetheless, coupling these particles with an

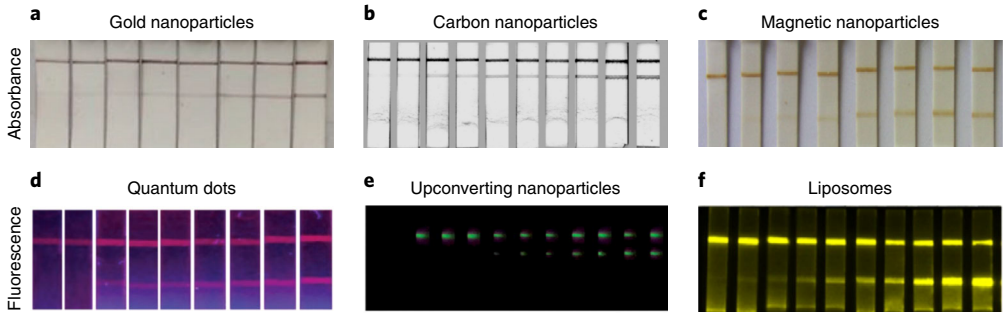

Fig. 2 | Examples of optical readouts of LFAs using different types of nanoparticles. The figure shows calibration assays for different targets (i.e., the different LFAs are not quantitatively comparable) using nanoparticles providing an absorbance value (gold nanoparticles (**a**)[196], carbon nanoparticles (**b**)[89] and magnetic nanoparticles (**c**)[127]) and others generating a fluorescence signal (quantum dots (excitation: 365 nm; emission: 540 nm; **d**)[197], upconverting nanoparticles (excitation: 980 nm; emission: 540 nm; **e**)[198] and fluorescence-loaded liposomes (excitation: 535 nm; emission: 600 nm; **f**)[116]). Panel **a** is adapted from ref. [196] with permission from Elsevier. Panel **b** is adapted from ref. [89] with permission from Elsevier. Panel **c** is adapted from ref. [127] with permission from Elsevier. Panel **d** is reproduced by permission of The Royal Society of Chemistry[197]. Panel **e** is reproduced by permission of The Royal Society of Chemistry[198]. Panel **f** is adapted from ref. [116] with permission from Elsevier.

Table 3 | Common labels used in LFAs and their advantages and disadvantages

Label	Advantages	Disadvantages
AuNPs	Qualitative naked-eye detection	Quantitative detection requires extra hardware
	Well-known conjugations	Relatively expensive if commercially bought
	Strong signal	
CNPs/CNTs	Qualitative naked-eye detection	Quantitative detection requires extra hardware
	More stable	Unspecific adsorption
	Cheaper than AuNPs	Weaker signal than AuNPs
	High signal-to-noise ratio	
Latex beads	Qualitative naked-eye detection	Quantitative detection requires extra hardware
	Resistant to chemical and physical damage	Less sensitive
	Cheaper than AuNPs	Weaker signal than AuNPs
	Multiple colors available	
QDs	Strong fluorescent signal	Requires extra hardware (UV light and reader)
	Multiple colors available	Higher toxicity
UCNPs	Strong fluorescent signal	Requires extra hardware (NIR laser)
	No UV source necessary	More expensive than QDs (they are made of rare materials)
	Multiple colors available	
Liposomes	Loading of multiple labels	Require extra hardware depending on the loaded label
	Easy conjugation	Delicate to pH and ionic strength
MNPs	Dual magnetic/colorimetric signal	Require non-optical reader for magnetic measurements
	High signal-to-noise ratio	
	Very sensitive	
	Possibility to incorporate sample before treatment and analyte before concentration	
AuNPs for thermal reading	Dual thermic/colorimetric signal	Require expensive non-optical reader and a laser
	High signal-to-noise ratio	
	Very sensitive	

CNP, carbon nanoparticle; CNT, carbon nanotube.

external reader may increase the reproducibility and provide the quantitative analysis required for more challenging applications.

- *Gold nanoparticles*. Since the 1980s[77–79], gold nanoparticles (AuNPs) have become the most widely used detection labels in LFAs. The reasons behind their popularity are that (i) their SPR produces a strong red color ideal for naked-eye detection[80], (ii) there are different synthetic methods that are able to produce AuNPs with different sizes and shapes[21,81], (iii) they have low toxicity, (iv) they can be easily functionalized either by nonspecific adsorption[19] or via covalent bonds[82–85] and (v) they are relatively stable. Given that AuNPs are the most

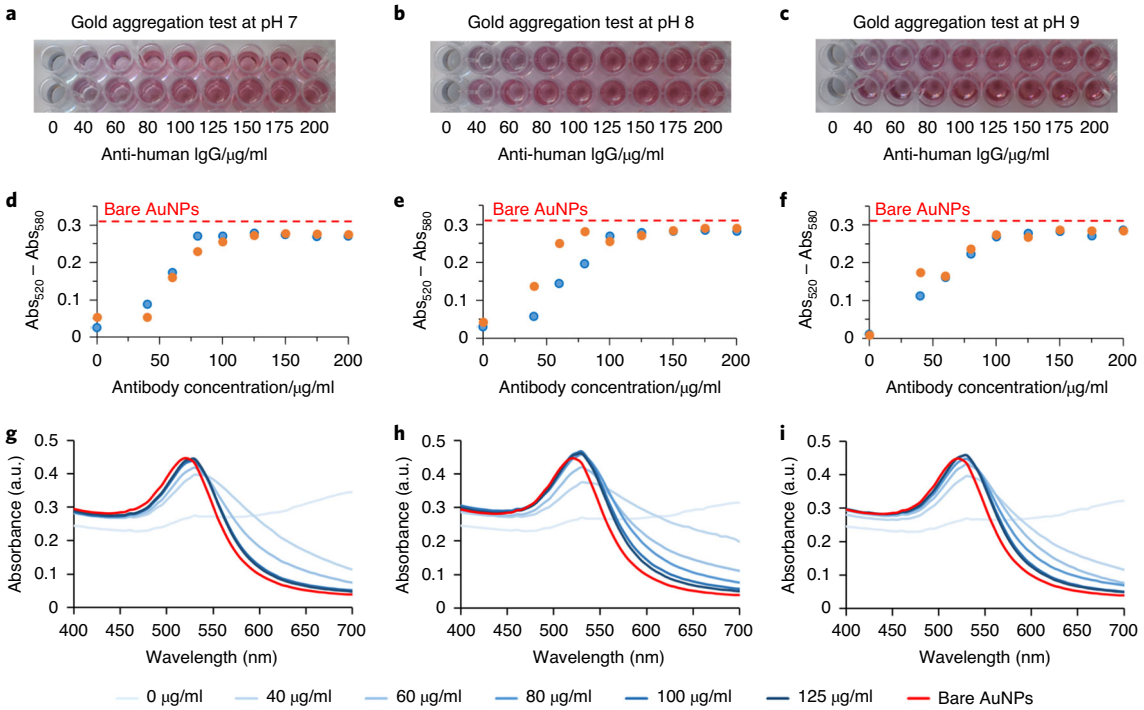

Fig. 3 | Example results of a gold aggregation test for 20-nm diameter AuNPs and anti-human IgG. a–c, Photos of the resulting gold aggregation test. Even by the naked eye, the color gradient after the different anti-human IgG concentrations is clear. **d–f**, Bar charts, relative to the photos in **a–c**, obtained by subtracting the absorbance value at 520 nm from the one at 580 nm[199]. This analysis allows for estimation of the minimum antibody concentration to give stable conjugates. The higher the calculated value the narrower the peak, indicating more monodispersed AuNPs. Abs, absorbance; a.u., arbitrary units. **g–i**, Spectra obtained for the different tested conditions confirm the bar chart results. It is important to note that the peak position for stable conjugates will be slightly shifted to higher wavelengths (in this case, 530 nm) due to the increased hydrodynamic diameter of conjugates (AuNPs + antibody) compared to that of bare AuNPs (in this case, 520 nm).

common labels in LFAs, in this paper, we propose an easy-to-optimize functionalization procedure (Box 2, steps 1–16; Fig. 3). In addition, we provide a step-by-step procedure for qualitative (by the naked eye) and quantitative (camera-based) detection of an AuNP-based LFA (Box 2, steps 42–55; Figs. 5,6 and 7). Troubleshooting guidance is provided in Table 4.

- *Carbon-based materials*. Recently, carbon nanoparticles[86–92] and carbon nanotubes[93,94] have provided an alternative to AuNPs. Although they do not have a plasmon resonance that provides as strong a signal as AuNPs, being black offers a stronger contrast to the white background of the nitrocellulose. In addition, they are cheaper to produce, less prone to aggregation and easy to functionalize.
- *Dye-loaded latex beads*. Another alternative to AuNPs are dye-loaded latex beads, as they are cheap and can be purchased in different colors[2,95]. In addition, they are less sensitive to chemical and physical damage[18]. However, they are more suitable for qualitative assays and clinical screening, since their limit of detection tends to be higher in comparison to AuNPs[72].

Fluorescent reading

The use of fluorescent labels is generally recommended for the detection of low target concentrations and/or application requiring quantitative results. However, this comes with a higher cost and the need for an external reader. Examples of suitable fluorescent nanoparticles are:

- *Quantum dots (QDs)*. In fluorescence-based LFAs, QDs are typically the most used labels[96]. When excited with UV light, they provide strong photoluminescence, whose emission peak can be tuned by changing the elemental composition and size of the QD. This also makes them ideal for multiplexed detection[97–100]. In addition, they can be easily conjugated to bioreceptors[101–104] and provide higher stability and resistance to photo-bleaching than organic dyes[105]. Nonetheless, their elemental composition may be toxic, their cost is generally higher than AuNPs and they require a UV lamp for excitation[96,106–108].
- *Upconverting nanoparticles (UCNPs)*. Since the early 2000s, UCNPs have been applied as labels in LFAs[109–111]. Their excitation wavelengths, which is in the near-IR range, do not produce auto-fluorescence of the membrane (which occurs when illuminated with UV light), and their strong emission in the visible region produces more-sensitive LFAs than those obtained using QDs[112]. However, the need for an expensive and bulky near-IR laser is not appropriate for many PoC applications, thus limiting the integration of UCNPs in LFAs[112–115].
- *Liposomes*. In an effort to increase the sensitivity of LFAs, the possibility of encapsulating fluorescent dyes into liposomes has also been explored. Besides carrying a high number of fluorescent dyes with the capability of producing a strong fluorescence signal, the possibility of tailoring the lipid bilayer composition allows for ease of functionalization of the liposome surface with bioreceptors[116–119]. However, the two main

limitations faced with liposomes as labels in LFAs are the complex synthesis techniques and poor stability.

Non-optical readings

LFAs with non-optical readout are also possible, and their use is comparable to that of fluorescence LFAs[120,121]. In fact, lower detection limits and more quantitative results can be achieved in comparison with fluorescence-based LFAs, but they require specific readers. Examples of nanoparticles suitable for magnetic and thermal readings are:

- *Magnetic nanoparticles (MNPs).* MNPs are versatile labels for LFAs, since they provide both an optical and a magnetic signal. Their dark color allows for their use as classical optical labels, and their magnetic field can be harnessed for easier functionalization (e.g., removing unbound bioreceptors without the need of centrifugation), for sample pretreatment (MNPs could be incubated with the sample and separated before their incorporation in LFAs to remove any contaminant)[122] and to provide a sensitive read out. In fact, while optical readouts rely mostly on the labels close to the surface of the membrane, measuring the magnetic field allows for the use of all the labels accumulated on the test line[72,123–130].
- *AuNPs for thermal reading.* There are few reports about the implementation of thermal methods on LFAs, which are based on the thermal radiation emitted by AuNPs after being excited by a laser. This strategy can be exploited to achieve lower limits of detection where colorimetric measurements cannot reach. Moreover, thermal contrast readings are highly reproducible over time with the same LFA strip. The main limitations of thermal contrast techniques are the need for both a laser and an IR camera. Nonetheless, recent efforts have been dedicated to the improvement of the portability of such setups[131,132].
- *Nanoparticles for electrochemical readings.* The use of an electrochemical output in an LFA can provide various amplification strategies and quantitative outputs[133–135]. Although there are just a few examples of this type of readout (especially those employing nanoparticles as electrochemical labels) in LFAs, we believe they will be more frequent during the next years[133,136]. In our opinion, the reasons behind their limited spread so far is the increased complexity in the fabrication of LFAs. Although there are various techniques that can be used (such as screen printing, inkjet printing, writing and pressing)[137–139] for the modification of membranes with electroactive materials, these approaches still necessitate extra steps and reagents during the fabrication process, in addition to the requirement of a dedicated reader.

Sample pad

The sample pad represents the portion of an LFA where the sample is loaded at the beginning of the test. This component has two key functions: (i) ensuring an even flow and (ii) the standardization of the buffer conditions of the sample. The material and design chosen for the sample pad can have a major influence on the overall system[18–20,140].

Characteristics of sample pads

The geometry and characteristics of the sample pad are important for the control of the sample flow and for the design of the final product (it will affect the shape of the housing cassette). In particular, the key parameters are:

- *Bed volume.* The bed volume, or void/dead volume, refers to the volume of air contained within the sample pad. This parameter can be used to calculate the total amount of liquid that is required to wet the pad. It controls the volume of sample that flows to the rest of the LFA and is directly proportional to the thickness, porosity and overall dimensions of the pad:

$$\text{Bed volume} = \text{Total volume of the pad} * \text{Porosity}(\%)$$

For example, for a pad measuring 5 cm long, 0.5 cm wide and 0.015 cm thick, with a porosity of 70%, the bed volume would be: 5 cm × 0.5 cm × 0.015 cm × 0.7 = 0.02625 cm^3 = 26.25 µl. It can also be expressed as volume over area, since different providers have different pad geometries; in this case, it would be 10.5 µl/cm^2.

- *Thickness.* The thickness of the pad not only influences the bed volume but also affects the consistency of the flow. For example, a thicker sample pad provides higher buffering capabilities as well as a slower and more stable flow. A slower flow generally produces a higher sensitivity of the LFA by increasing the probability for the successful biorecognition of the target by the labeled bioreceptor. A thick pad may also be compressed by the housing cassette, leading to a decrease in the amount of sample absorbed and a reduced flow speed. On the other hand, thin sample pads require less sample volume, but have lower buffering and faster flow speeds, which may negatively affect the wetting of the following pads and decrease the sensitivity of the test.
- *Absence of extractable material.* During the fabrication of the sample pad, manufacturers may include chemicals (referred to as extractable material) to confer particular properties on the material. For the design of an LFA, it is important to verify that there is no release of unwanted chemicals that may affect the flow or the biorecognition of the target.
- *Particle retention rating.* The particle retention rating refers to the particle size that the sample pad is able to remove, allowing a proper filtration of the sample. If the chosen sample pad does not provide the desired particle retention rating, it is possible to incorporate an extra pad (e.g., blood filtration membranes).

Types of sample pads

There are two main types of material used in commercially available sample pads: cellulose fibers and woven meshes. Sample pads made of cellulose fibers tend to be thicker (≥250 µm) and cheaper, but are also weaker for handling, especially when they are wet (making the fabrication more delicate). They typically have bigger bed volumes (≥25 µl/cm^2) and have higher tolerance toward the chemicals present in the sample pad buffer. Sample pads made of woven meshes, such as glass fibers, have good tensile strength and enable even distribution of the sample over the conjugate pad. In addition, woven meshes can also act like a filter for removing particulates from the sample (e.g., Whatman LF1 and GE Healthcare Life Sciences GF/DVA made of glass fiber, Whatman Fusion 5 made of a polyvinyl alcohol–coated glass fiber and the Pall Vivid Plasma Separation membrane made of asymmetric polysulfone), avoiding the blockage of further pads in the remaining LFA, and are able to retain minimal amounts of sample, thanks to their low bed volumes

(≤2 μl/cm^2). On the other hand, they tend to be more expensive, are sometimes more difficult to cut than cellulose fibers and can be affected by chemicals used during the fabrication.

In general, developers should choose the sample pad based on the type of analyte they want to detect, the amount of sample available and the type of sample. In addition, if the analyte is in the micron size range (i.e., bacteria and cells), then the sample pad should have a high bed volume (cellulose fibers) that allows flow of the analyte along the LF strip. Similarly, for a sample requiring consistent buffering, a thick sample pad should be preferred (cellulose fibers). In contrast, for the analysis of small volumes of samples, a low bed volume and a thin sample pad (woven meshes) should be the ideal choice. Although these general guidelines could help to short-list the best materials, we still recommend that developers try different types of pads.

Sample pad buffer and preparation

In addition to filtering out impurities, the sample pad corrects the sample composition by adding reagents that confer the appropriate pH, ionic strength, viscosity and blocking capabilities. To achieve this, the sample pad is generally soaked in a dedicated buffer and further dried, before its application in the LFA strip (Box 2, steps 27 and 28). Looking at the sample pad buffer composition, we find four main components:

- *Buffering agents*. The type and concentration of buffering agents will determine the pH and ionic strength of the solution for the whole duration of the assay. This affects not only the reproducibility of the assay (by creating the same conditions for different samples), but also the sensitivity and specificity of the test itself (pH and ionic strength can affect the interaction between the receptor and target as well as nonspecific binding; this should also be considered for other buffers used in the LFA, such as the running or washing buffers). The most-used buffers are phosphate (pH range between 5.8 and 8)[141,142], Tris (pH range between 7.5 and 9)[143,144], HEPES (pH range between 6.8 and 8.2)[57] and borate (pH range between 8 and 10)[145]. Their concentration depends on the specific application, but it generally varies between 10 and 100 mM, where higher concentrations are used for more complex and variable samples.
- *Detergents*. The use of detergents in the sample pad buffer has two main functions: (i) minimizing the nonspecific binding (disrupting weak ionic and hydrophobic bonds) and (ii) facilitating the flow of the detection labels along the different pads. Common detergents used in the sample pad are SDS (concentration ranging between 0.05% and 0.5% (wt/vol)), Tween 20 (concentration ranging between 0.01% and 0.1% (vol/vol)) and Triton (concentration ranging between 0.05% and 1% (vol/vol)).
- *Blocking agents*. Together with detergents, the use of blocking agents in the sample pad buffer can minimize the formation of nonspecific bonds, making the LFA more specific. Furthermore, by adding the blocking agent onto the sample pad, blocking of the membrane may not be required, making the overall fabrication easier and faster. The most commonly used blocking agents are BSA (concentration ranging between 0.01% and 0.1% (wt/vol)), milk (concentration ranging between 0.01% and 0.1% (vol/vol)) and casein (concentration ranging between 0.1% and 2% (wt/vol)). Chaotropic agents, such as polyvinyl alcohol (concentration ranging between 0.1% and 1% (vol/vol)), polyvinylpyrrolidone (concentration ranging between 0.3% and 1% (vol/vol)) and polyethylene glycol (concentration <0.5% (vol/vol)), are sometimes also added into the sample pad buffer to prevent nonspecific interactions; however, this strategy is less commonly used[146].
- *Preservatives*. Finally, preservatives such as sodium azide (concentration ranging between 0.01% and 0.05% (wt/vol)) could be used in commercial tests to avoid microbial contamination on the LFA strip.

Generally, the drying of the sample pad follows a less delicate procedure than that for the drying of the conjugate pad or the membrane. This is mainly due to the absence of delicate reagents, such as antibodies and nanoparticles, in the sample pad. The most common drying method is placing the sample pads in an oven at 37 °C, but this can be increased to 45–60 °C. Alternatively, the sample pads can be dried by vacuum drying.

Conjugate pad

The conjugate pad is the second pad to be encountered by the sample. It has three main functions: (i) preserving the dried conjugated nanoparticles for detection, (ii) releasing them upon wetting by the sample and (iii) providing the first interaction between the labeled bioreceptor and the target. Given its key role in the LFA, preparation of the conjugate pad is one of the most critical stages during fabrication of the device. Overall, the conjugate pad should provide low nonspecific binding (to avoid the retention of the nanoparticles or the target on the conjugate pad), a consistent flow and bed volume (achieving a homogenous and reproducible flow along the width of the membrane is essential to obtain reproducible results) and mechanical strength without extractable material (the conjugate pad must resist the fabrication process and the housing without releasing any material that can block the membrane or interfere with the signal generation)[18–20,140].

Types and characteristics of conjugate pads

The most-used material for the conjugate pad is glass fiber, although cellulose and polyester can also be used. The choice of the conjugate pad material should take into account several factors such as thickness, bed volume and resistance to nonspecific binding. In particular, cellulose pads provide higher thickness (300–1,000 μm), followed by glass fiber (100–500 μm) and polyesters (100–300 μm). As mentioned for the sample pad, a thicker material generally means a higher bed volume (assuming similar pore size). This in turn allows for the storage of a higher amount of nanoparticles for detection, a slower flow and a higher sensitivity. At the same time, it is also related to a weaker mechanical strength of the material when it is wet.

Conjugate pad buffer and preparation

The conjugate pad buffer functions to maximize the stability of the particles and to completely release them upon re-wetting by the sample. In the conjugate pad buffer composition, we find two main components (besides the particles):

- *Buffering agents*. Given that most nanoparticles used for detection in LFAs are colloidal suspensions, their stability is

generally affected by the ionic strength of the solution. Considering that the nanoparticles will undergo a drying process during the fabrication of the LFA (which produces a temporary increase in the salt concentration), it is recommended to start with a low ionic strength. For example, one of the most common buffers used for this purpose is borate buffer at 2–5 mM. It is important to note that, during the assay, it is the sample pad buffer that has the major role on the buffering of the overall test.

- *Stabilizing and re-solubilization reagents*. The key components of the conjugate pad buffer are sugars, in particular sucrose and trehalose. They have two main functions: (i) preserving the native conformation of dehydrated proteins (the hydroxyl groups of sugar molecules replace the water around the protein upon drying) and (ii) their quick re-solubilization upon wetting[147]. Typically, they are used at concentrations ranging from 1% to 10% in volume[148].

Once a suitable buffer has been chosen, the bioreceptor-nanoparticle conjugate can be loaded into the membrane by either air jet dispensing or by an immersion process (Box 2, steps 29–39). Air jet dispensing is the most reliable non-contact method to deliver the particles, as it provides quantitative coverage all over the membrane. The immersion method, on the other hand, is used when the air jet method is not possible; however, the major drawback is that the coverage is not uniform and may lead to high sensor-to-sensor variability[143].

The drying process is crucial to maintain the stability of the dried bioreceptor-nanoparticle conjugate and determines the release efficiency from the membrane. For example, failing to completely dry the conjugate pad may generate a syrup-like solution unable to run through the membrane. There are two ways to dry the conjugate pad upon loading: hot air and vacuum drying[19]. For mass production of LFAs, hot air is the most convenient method (given its ability to process a high quantity of conjugate pad and its lower cost) and is typically fixed at 37 °C to not affect the stability of the bioreceptors[34,144]. In smaller laboratories or when mass production is not required, vacuum drying may be the preferred method as it is not a heat-induced drying process and therefore does not affect the stability of the bioreceptors (although it requires more expensive and delicate equipment).

Membrane

The membrane (also called detection pad) is the part of the LFA strip where the signal is generated. The key characteristics of the membrane are that it should (i) facilitate a homogenous flow, (ii) provide a solid functionalization for capturing the bioreceptor and (iii) show low nonspecific binding.

Types and characteristics of the membrane

Commercial membranes are generally defined by their capillary flow time, which is the time required for the sample front to cover the membrane length (generally 4 cm), and is generally expressed as s/4 cm. A few manufacturers classify their membranes based on their pore sizes, and, in that case, the conversion of pore size to capillary flow time is roughly: 8 μm = 135 s, and 6 μm = 180 s. In general, the higher the capillary flow time, the slower the flow speed. This parameter is crucial not only for the overall duration of the assay, but it also has a fundamental role in defining the sensitivity and specificity of the LFA. High capillary flow times allow for a longer interaction time between the target molecule and the bioreceptor, thus increasing the sensitivity of the test[149]. At the same time, high capillary flow times also increase the chance for nonspecific binding to happen. Therefore, it is crucial to evaluate the membranes, with particular attention to the different capillary flow times, during the development of an LFA.

The membrane material defines the type of interactions that govern the functionalization of the membrane with the capture bioreceptors (both for the test and control lines). Nitrocellulose is the most commonly used membrane due to its low price, its strong binding to proteins (including antibodies, the most used type of bioreceptors) and its tuneable wicking properties (obtaining different capillary flow times and the possibility of changing surfactant content)[150]. Regarding the other types of membranes, polyvinylidene fluoride is mainly used for water filtration and western blot thanks to its broad solvent compatibility, low background and superior staining capabilities. Similarly, nylon is also mainly used for filtering aqueous and organic solutions because it is strong, flexible, hydrophilic and solvent resistant. Finally, because of its hydrophilicity and extremely low protein binding, polyethersulfone is generally used to remove micro/nanoparticles, bacteria and fungi from the sample.

Immobilization buffer

Overall, membrane functionalization with the capture bioreceptor occurs via non-covalent binding (e.g., for nitrocellulose, there are mostly electrostatic and hydrophobic interactions)[151], and as such, it is important that the immobilization buffer is optimized accordingly. In this respect, the immobilization buffer has to maximize the capture bioreceptor adsorption on the membrane, maintain the capture bioreceptor reactivity and not alter the flow properties of the membrane. Looking at its composition in more details, we find four main components:

- *The buffering agents*. The ideal buffer should maintain the stability of the capture bioreceptor and promote its binding to the membrane. For this reason, buffers with low ionic strength (10 mM) and a pH between +1 and −1 unit of the isoelectric point of the capture bioreceptor are preferred. Buffer compositions with high salt concentrations may screen the electrostatic interactions between the membrane and the capture bioreceptor. In addition, slightly varying the pH from the isoelectric point of the bioreceptor ensures proper solubility without affecting its tertiary structure. The two most common buffers used for this purpose are ammonium acetate and phosphate buffers.
- *Stabilizers*. As mentioned for the conjugate pad buffer, the presence of sugars can help stabilize the capture bioreceptor once the membrane is dried. For this reason, low concentrations of lactose (0.1% (wt/vol)) or trehalose (1% (wt/vol)) can be included, and their concentration should be carefully optimized to avoid losing bioreceptor activity upon re-solubilization.
- *Alcohols*. Alcohols are also included in the immobilization buffer due to their ability to reduce the solution's surface tension,

viscosity and static repulsion; enable faster drying times; and improve the binding of the capture bioreceptor to the membrane. The most commonly used are methanol, ethanol and isopropanol at concentrations between 1% and 10% (vol/vol).

Membrane striping

The immobilization buffer composition and the membrane material define the type and efficiency of membrane functionalization with the bioreceptor. The striping strategy itself (i.e., the deposition of the bioreceptor onto the membrane) is crucial to define the width of the test and control lines (Box 2, steps 17–24). As this is a fundamental aspect with respect to the reproducibility of the LFA, the striping should be performed using automated dispensers, allowing for precise control over the flow rate and the speed (thus, the deposition amount of bioreceptor), as well as the positioning of the lines onto the membrane. There are two types of automated dispensers: contact and non-contact. Although both types provide similar results, different precautions must be taken for each instrument. For contact dispensers, it is important to verify that the dragging of the nozzle does not produce indentations, or grooves, on the membrane. For the non-contact method, the dispensing height should be optimized for membranes of different thicknesses.

Looking in more detail at the striping process, we find four main parameters:

- *Bioreceptor concentration*. The capture bioreceptor concentration will determine the maximum signal achievable by the LFA. Intuitively, the more concentrated the bioreceptors on the test line, the higher the density of labeled nanoparticles is that can be achieved. In the case of immune sandwich assays (Box 1), it is generally recommended to use an antibody concentration of ≥1 mg/ml in the dispensing solution (Box 2, step 19). For competitive assays (Box 1), where the presence of target (often, but not limited to, small molecules presenting a single binding site: atoms, toxins, pesticides or peptides) decreases the signal, the capture bioreceptor concentration should be ~0.1 mg/ml up to 1 mg/ml. In this case (or if the capture bioreceptor is particularly expensive, or the use of a highly concentrated solution is not feasible), it is often necessary to compensate the low bioreceptor concentration with a complementary protein, such as BSA, to raise the overall protein concentration in solution. This precaution is necessary to maintain the structure and functionality of the bioreceptor over time, as low concentrations can induce protein denaturing and loss of binding activity.
- *Flow rate and speed*. The dispensing flow rate defines how much liquid is dispensed over time (i.e., how much bioreceptor-containing solution is dispensed) and is generally defined in µl/cm. The higher the flow rate, the larger the dispensed volume (for a fixed area) and the wider the striped line will be. The speed defines the distance travelled by the nozzle over time and is generally expressed in mm/s. Thus, for a fixed flow rate, the slower the speed the higher the volume of bioreceptor-containing solution that is dispensed. During the fabrication of an LFA, the developer must optimize and balance these two values to obtain reproducible and well-defined lines. Generally, it is preferred to obtain narrower lines since this allows the use of higher bioreceptor concentrations and is more cost effective. For antibodies, and assuming the use of a nitrocellulose membrane with average capillary flow time (120 s/4 cm), the starting parameters are typically 1 µl/cm for the flow rate and 20 mm/s for the speed (Box 2, step 22).
- *Position and size*. Besides affecting the geometry of the housing cassette (in particular, the position of the reading window), the position of the test line also contributes to the sensitivity of the LFA. The further it is placed from the conjugate pad, the more time is allowed for the labeled detection bioreceptors and the target to interact, thus increasing the number of possible immune complexes to be captured onto the test line[152]. The only requirement for the control line is that it must be positioned after the test line, since it should confirm successful flow of the sample front until the end of the strip. Usually, the test line is dispensed 12–13 mm from the origin of a 60-mm strip, while the control line is 4 mm behind the test line. In the case of a multiplexed sensor, several test lines can be dispensed onto the same membrane, but there should always be at least a 2-mm spacing between them. For a deeper understanding of the best test line position, we refer the reader to the work from Ragavendar and Anmol[153].
- *Drying*. Similar to the conjugate pad, the presence of proteins (including antibodies) on the membrane requires delicate drying, as high temperatures may denature the bioreceptors. The general conditions adopted are for 2 h at 37 °C (Box 2, step 24).

Blocking conditions

Although commercial membranes can generally directly be striped with the capture bioreceptors, in some cases it is necessary to further treat them with a blocking agent (Box 2, step 25). However, generally speaking, blocking of the membrane should not be performed unless it is strictly necessary (i.e., when the blocking agents added to the sample or conjugate pad are not enough). Although blocking of the membrane decreases nonspecific signals, from a fabrication point of view, this step is quite cumbersome, requiring additional reagents, incubation and drying steps, and potentially affecting the flow of the sample. Consequently, this may affect the reproducibility and the overall analytical performance of the LFA. However, if blocking the membrane is required, it should always be performed after the striping and drying of the capture bioreceptors; otherwise, the blocking agent hinders the functionalization of the membrane. Common blocking agents are 1–2% (wt/vol) BSA, 1–2% (wt/vol) IgG, 0.1–0.5% (wt/vol) gelatine, 1–2% (wt/vol) casein, 0.5–1% (wt/vol) polyvinylpyrrolidone (8–10 kDa) and 0.1–1% (wt/vol) polyvinyl alcohol (8–10 kDa). The choice of the blocking agent depends on the type of membrane, the sample and the capture bioreceptor. Generally, the blocking agent should be smaller than the capture bioreceptor, so as not to induce steric hindrance that may affect its binding to the target analyte. PBS (0.01 M, pH 7.2–7.4) is the most commonly used blocking buffer. For blocking, the membrane is completely immersed in the blocking solution for 5–10 min and immediately washed (at least twice) with a weak buffer (e.g., 5–10 mM PBS, pH 7.2–7.4 with 0.005–0.01% (wt/vol) SDS) to remove

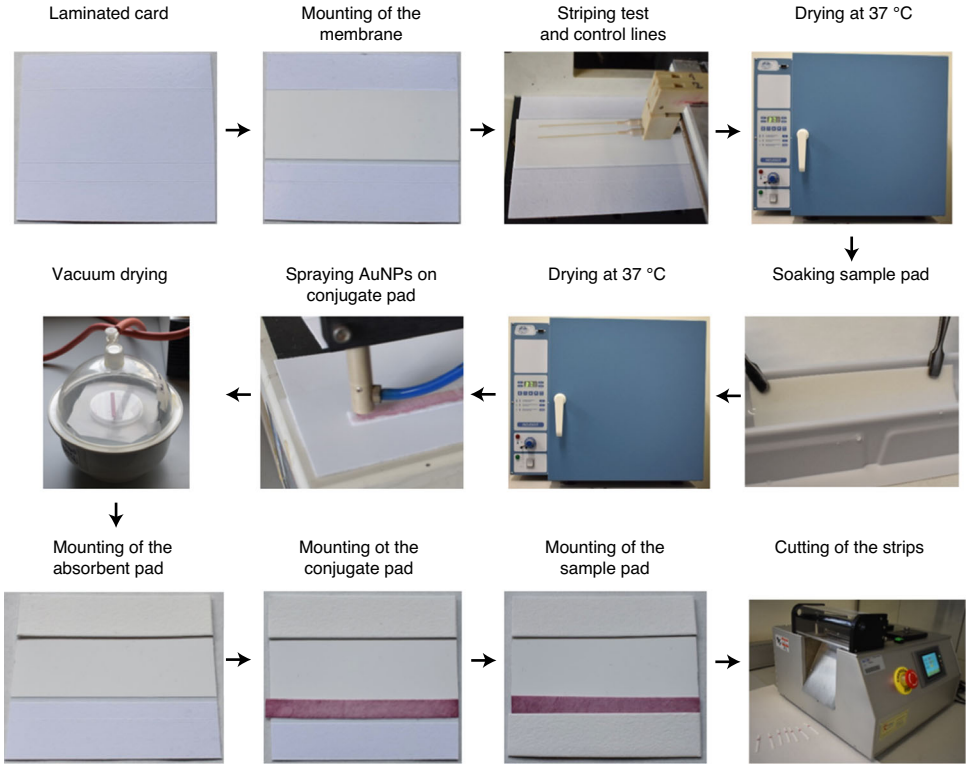

Fig. 4 | Step-by-step fabrication of an LFA for the detection of human IgG. For 'Laminated card', 'Mounting of the membrane', 'Striping test and control lines' and 'Drying at 37 °C', see Box 2, steps 17–26. For 'Soaking sample pad' and 'Drying at 37 °C', see Box 2, steps 27 and 28. For 'Spraying AuNPs on conjugate pad' and 'Vacuum drying', see Box 2, steps 29–39. Finally, for 'Mounting of the absorbent pad','Mounting of the conjugate pad', 'Mounting of the sample pad' and 'Cutting of the strips', see Box 2, steps 40 and 41.

excess blocking reagents (Box 2, step 25). Finally, the membrane is dried using the same conditions used after striping.

Absorbent pad

The last pad in an LFA is the absorbent pad, and its role is to control the volume of sample that a strip can take. In the absence of the absorbent pad, once the liquid reaches the end of the membrane, the flow stops and the liquid evaporates homogenously along the strip. This means that all the labels that did not reach the last part of the detection pad can accumulate on the strip and can increase the background noise. In contrast, the presence of an absorbent pad ensures that all the labels reach the end of the strip. The dimensions of the absorbent pad should be evaluated based on the volume of liquid that must pass through the membrane. Thus, for example, if the LFA requires the use of a washing buffer, then the absorbent pad should provide enough bed volume to guarantee the complete washing of the membrane (this can be achieved either using a material with a high bed volume or increasing the size of the absorbent pad). The absorbent pad does not require any special handling during LFA fabrication (Box 2, step 40; Fig. 4), and although its use is generally recommended, considerations such as its cost and its implementation in the LFA geometry (its incorporation requiring a housing cassette that is able to accommodate it) should be evaluated by the developer[18–20,140].

Assembly of the LFA

The assembly of the different pads and membrane on the strip (Fig. 4) is the final step before storing. Although sticking the pads and membrane on the supportive laminated card might seem trivial, it is actually an important step that will ensure the homogenous flow of the sample along the strip and batch-to-batch reproducibility. The developer should ensure contact between the sequential pads and their complete wettability to move all the reagents along the strip. Most laminated cards come with release liners that help to position the different pads always at the same distance. This is convenient if the sizes of the different pads and the relative release liner are the same. There are also dedicated laminators commercially available, which would improve consistency in the fabrication process. A detailed step-by-step procedure for assembling a standard sandwich LFA is described in steps 40 and 41 of Box 2.

Finally, the LF strip may be inserted in the housing cassette. It is possible to purchase pre-made housing cassettes from most of the pad/membrane providers, although in this case, the width of the LF strip must be adapted to the width of the cassette (this assuming that the length and height are compatible given that they are produced by the same company). Alternatively, LFAs with non-common geometries (e.g., using materials from different providers, or having dimensions not compatible with the cassettes) or requiring special functionalities (i.e., the application of the sample and a running buffer at different positions of the LF strip, or requiring the docking of the cassette to a dedicated

reader) may require the design of a dedicated cassette. In this case, we recommend testing different cassette geometries using a 3D printer, which provides the freedom to vary several parameters at a low cost. Once the developer finds the final design, the cassette can be mass-produced by specialized companies. Overall, once designing a housing cassette, the developer should consider three main aspects. First, the cassette should keep the LF strip in place (i.e., preventing it from flipping over or moving inside the cassette), without compressing or damaging the pads/membrane (this would affect the flow of the sample). Second, the cassette should have the hole to apply the sample positioned in the bottom part of the sample pad, so as to ensure the flow of most of the sample toward the membrane. Third, the reading window of the cassette must allow the user or the reader to easily visualize both the control and the test line(s).

Single-membrane LFA

So far, we have described the materials and features of the different membranes in a typical LFA strip. Alternatively, there is one membrane marketed by GE Healthcare that simplifies the manufacturing process, as well as minimizing costs: Fusion 5[154]. This unique glass fiber–based membrane with proprietary technology facilitates production of LF strips, because it can adopt any of the roles of the different pads and membranes needed for a single LFA in just one single device. In general, Fusion 5 overcomes several problems when manufacturing LF strips, such as compatibility and contact issues between the membranes. When working with complex samples such as blood, it can act as a separator, obtaining a serum with a similar yield compared to conventional centrifugation procedures within 1 min after application of the blood drop. It also can act as a conjugate pad due to its composition and permanent negative charge, which enables the release of the conjugate to the detection pad. As a detection membrane, Fusion 5 does not need to be blocked to avoid unspecific adsorption. Two major drawbacks of the Fusion 5 are the need for carrier beads to load the bioreceptors of the test and control lines and its low capillary flow time (38 s/4 cm, a relatively fast flow compared with some nitrocellulose membranes), which may reduce the sensitivity of the test in comparison with other types of membranes. As of March 2020, we did not find any scientific articles describing the development of an LFA using solely Fusion 5; instead, we found references using Fusion 5 as part of LF strips or more complex structures[155–162].

Non-conventional materials

Other interesting low-cost alternatives to conventional LFA membranes, such as cotton threads, cellulose and glass capillaries, have been described in the past few years. For instance, cotton threads are attractive for LFA development because of their flexibility and wicking properties, which allow the control of smaller sample volumes[163–166]. Cellulose fibers (i.e., paper) have been extensively used for microfluidic paper analytical devices and some for LFA, because of their ubiquitous availability, biodegradability and patterning capabilities[167]. Although they are a convenient option for diagnostics performed in low-resource settings, their major drawback is the need for a chemical modification to guarantee the immobilization of bioreceptors. Finally, glass capillary tubes can also be used to take advantage of their transparency, smooth surface and chemical inertness. These characteristics make them especially useful for minimizing nonspecific binding by contaminants present in the sample matrix[168,169].

Storage

To ensure that the analytical performance of the LF strip remains constant over time and within different applications and environmental conditions, the storage conditions of LF strips play a vital role. There are three main components that can affect the stability of an LF strip: the bioreceptors, the membrane and the label.

In most cases, the bioreceptor will be the limiting factor for the stability of the strips. Regarding bioreceptor stability, we need to distinguish between stable DNA molecules, which also include aptamers, from more delicate proteins, such as antibodies. If properly dried, DNA molecules can withstand a wide range of temperatures and storage conditions. To maximize the shelf life of proteins, dry and cool conditions are required (4 °C inside sealed bags with desiccants)[170]. If other proteins are included on the strips (e.g., BSA as a blocking agent in nitrocellulose), then the same storage considerations should be taken into account. Particularly delicate bioreceptors may also require the addition of stabilizers (such as sugars, proteins, agars and gelatines[171]) to the relative buffers (e.g., whey would be striped together with the capture bioreceptor or included in the conjugate buffer). In addition, it should be considered that some surfactants used on LF strips to improve the flow across the paper or the release of the label particles may reduce the lifetime of the proteins. Second, the membrane itself has an expiration date. Deteriorated nitrocellulose shows a yellowish color, produces a sour smell and might generate faint lines after performing the assay. To maximize its lifetime, nitrocellulose should be stored in dry conditions and protected from direct light (i.e., in a zipper bag with dessicants). Finally, the stability of the detection label often depends on the nature of the label itself: properly modified (e.g., coated with a blocking protein during conjugation) and dried particles in glass fiber should not have any stability issues, whereas enzyme-based or dye-loaded particle labels may require refrigeration to preserve their activity. LF strips should not be frozen.

Assay evaluation

Qualitative evaluation

When thinking of an LFA, the first thing that comes to mind is the presence or absence of the line in a pregnancy test (Fig. 5a). This intuitive and qualitative analysis done by the naked eye is the reason for LFA popularity, and it is ideal for the discrimination between the presence or absence of a particular condition, such as pregnancy. Figure 6 shows qualitative analysis of LFAs for detection of human IgG as reported in Box 2, steps 42–44.

Semi-quantitative evaluation

A different approach for reading an LFA by the naked eye relies on the use of barcode-style LFAs, where the number and the intensity of multiple test lines facilitate a semi-quantitative

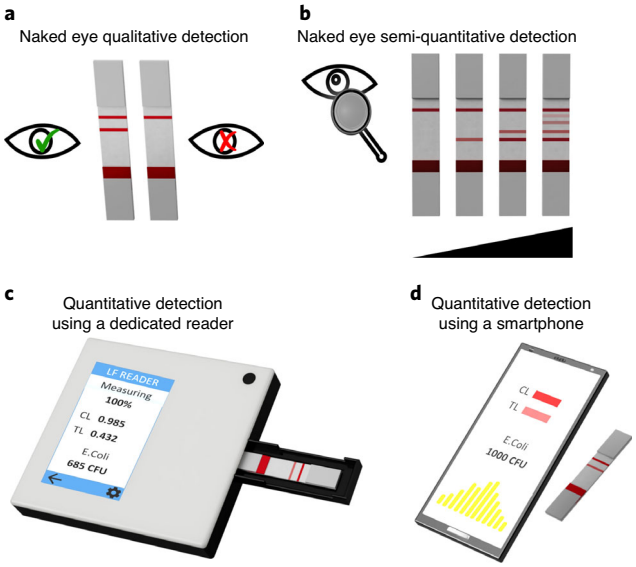

Fig. 5 | Different types of readouts of LFAs. a, Most LFAs are designed to give a qualitative (yes or no) response ideal for naked-eye detection by non-specialized users (e.g., the pregnancy test). **b**, LFAs can also be designed to provide semi-quantitative results. This type of reading is strongly dependent on the fabrication of LFAs, when the developer needs to evaluate how different parameters can result in a graded sensor response. **c**, The use of dedicated readers can make LFAs fully quantitative devices. Although most readers record an optical response, it is also possible to have magnetic and thermal readers. **d**, More recently, smartphones are also being used as LFA readers (especially when coupled with an external platform to guarantee constant lighting) or as user interfaces (receiving the LFA results via WiFi or Bluetooth).

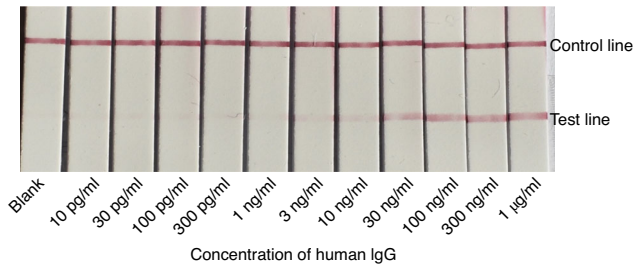

Fig. 6 | Qualitative analysis of LFAs for the detection of human IgG. The intensity of the test line increases with the concentration of target.

reading (Fig. 5b)[172,173]. These kinds of strips can be useful in three main scenarios: (i) when the concentrations of two or more analytes need to be assessed (i.e., the user can observe and compare the signals obtained for the different analytes and quickly verify if any of the analytes has a higher or lower concentration than the other), (ii) for the detection of a defined target concentration threshold (a measurable line appears if the concentration of an analyte is at least at the threshold value) and (iii) to group target concentrations into different categories based on concentration ranges (i.e., ranges of concentrations can be represented by using different lines). The latter scenario is useful for the detection of biomarkers, which are of interest just above or below a defined concentration, such as *Escherichia coli* in urine.

Quantitative evaluation

In recent years, the development of dedicated readers and smartphones has facilitated the quantitative analysis of LFAs (Fig. 5c,d) (Box 2, steps 45–55; Fig. 7)[174,175]. To achieve quantification, the fabrication process must provide highly reproducible strips (i.e., the developers and test manufacturers must strictly ensure that the LFA production is extremely rigorous; otherwise, the test result can greatly differ from different batches of LFA) and an accurate calibration curve to be used as a standard. The use of a dedicated reader is still preferred to obtain accurate measurements, as it minimizes the effect of ambient light on the signal intensity (to obtain a proper quantitative result, the measurement should be performed using the same light conditions as the original calibration, therefore the need of a fully closed box with integrated light sources). Hybrid systems where a smartphone is coupled to a special support also provide excellent performances[176,177].

Multiplexed evaluation

The detection of several targets at the point of care is highly desirable, for example, for drug screening, diagnosis of infectious diseases and monitoring of pesticides. Although the fabrication of LFAs for analysis of multiple targets is particularly challenging (i.e., higher cost, longer optimizations, possible cross-reactivity between biomolecules, etc.), there are some successful examples of this type of sensor[3,178–184]. In particular, for a few targets (approximately <10 different analytes), the readout could look like a barcode assay (where each line represents a specific analyte); for a high number of targets (>10 different analytes), the readout would look like a microarray (where each dot represents a specific analyte). Overall, the higher the number of lines or dots to analyze the more challenging is the naked-eye reading; thus, the use of a dedicated reader is recommended.

Iterative LFA development

As described, an LF strip is composed of various materials and reagents that are carefully interconnected to produce a sensor with the aim of being easy to use yet still highly sensitive and specific. The most challenging and complex task during the development stage is tuning the different parameters and components to achieve the best sensing performance. Although there are groups working on computational modeling to facilitate the optimization of LFA[17,185,186], this approach is not yet widely implemented because it requires modeling and programming skills that are not always present in research groups and because of the lack of availability of specific software.

More generally, in research and development (R+D) laboratories, the optimization of an LFA relies on an iterative approach of trial and error, as described by Hsieh et al[16]. As schematized in Fig. 8, the developer first defines the analytical performance, usability and cost required by the specific application. Then, on this basis, there is the first screening (using standard techniques such as ELISA and SPR) of bioreceptors and analytes, obtaining a short list of the most promising combinations. The resulting bioreceptors are then conjugated to

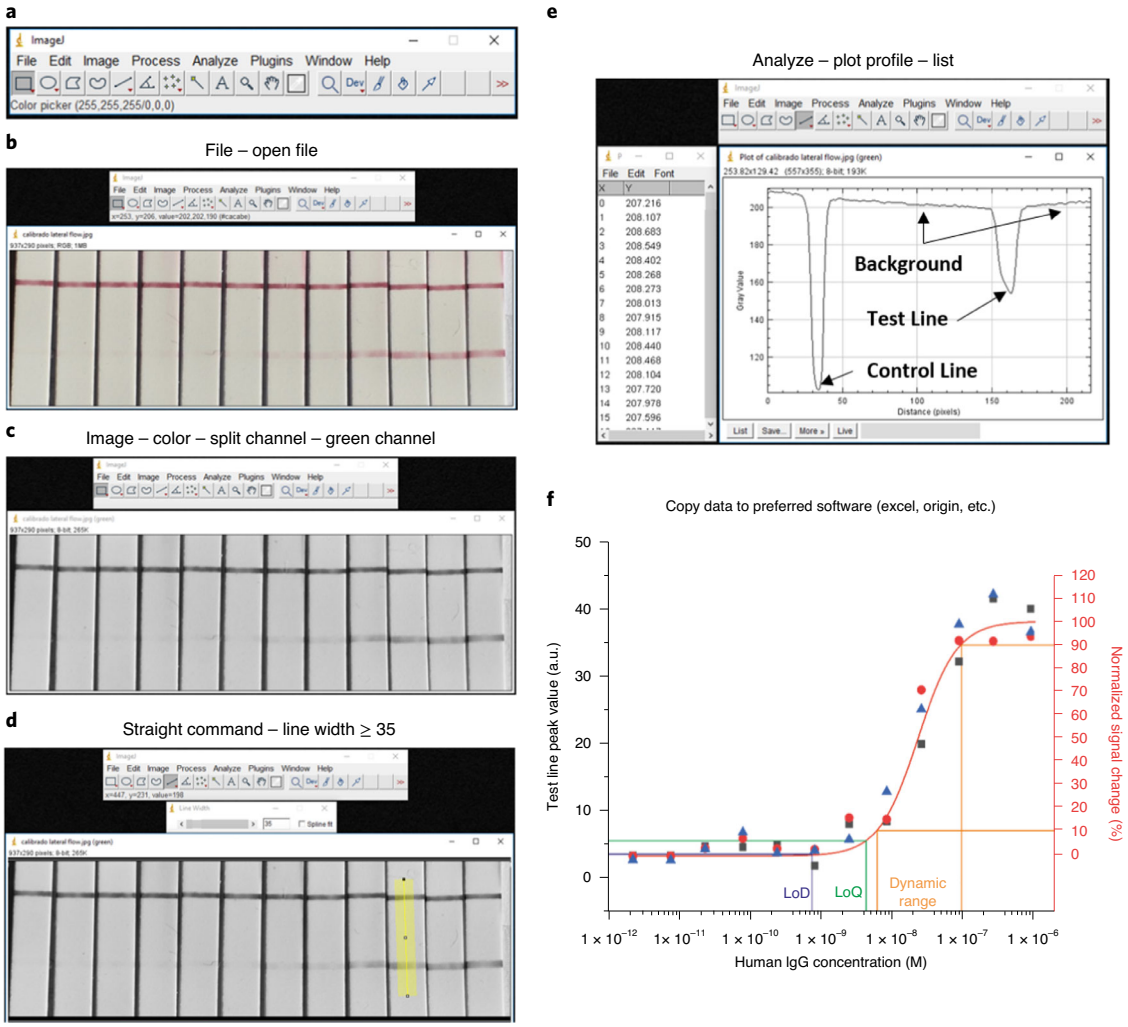

Fig. 7 | Quantitative analysis of an LFA using ImageJ and fitting the results to a four-parameter logistic curve (sigmoidal curve). a, Open the ImageJ software (Box 2, step 48). **b**, Open the file containing the photo of the strip(s). **c**, For LFAs employing red labels (i.e., AuNPs), the use of the green channel maximizes the sensitivity of the analysis (Box 2, step 49). The use of the straight command (**d**; Box 2, step 50) followed by the plot profile (**e**) allows the representation of the signal profile along an LFA strip (Box 2, step 51). For more reliable results, we recommend using a line width that covers most of the strip. From the plot profile, it is possible to extract the values and use data analysis software to calculate the peak value of the test line (Box 2, steps 52 and 53). It is obtained by subtracting the background signal from the peak value. **f**, The data must then be plotted against the target concentration, in this case, using a four-parameter logisitic curve (a sigmoidal curve). It is then possible to carry out statistical analysis such as calculating the limit of detection (LoD), the limit of quantification (LoQ) and the dynamic range (orange lines) (Box 2, steps 54 and 55). This graph was obtained analyzing three (n = 3) independent LFAs for each target concentration. The fitted curve (obtained using Origin 2018 64-bit and presented as value ± standard error) corresponds to the following equation: y = start + (end - start) × xˆn/(kˆn + xˆn), with start = 3.45 ± 0.25, end = 38.18 ± 3.12, k = 2.28 × 10^{-8} ± 8.41 × 10^{-9} and n = 1.58 ± 0.57. The reduced χ^2 = 2.68, R^2 = 0.97 and the adjusted R^2 = 0.96.

the nanoparticles, and the stability of the resulting conjugates is verified. At this point, developers use the half stick format (made of membrane and absorbent pad) to evaluate the combinations of membranes, blocking agents, running buffers, striping conditions and conjugates. If the original goals are met, developers use the 3/4 stick format (made of conjugate pad, membrane and absorbent pad) to evaluate the optimal preparation of the conjugate pad as well as the effect of the real sample matrix on the assay performance. Finally, there is the incorporation of the sample pad (and for commercial applications also the housing cassette) to evaluate the overall sensing performance. Although this approach for LFA optimization heavily relies on trial and error, it is still time and cost efficient. It is important to note, as we previously mentioned, that this is an iterative process, meaning that optimization steps might have to be repeated to compensate for changes done further down the optimization procedure.

Costs, patents and production

The estimation of the cost of an LFA depends on the development phase of that particular test: R+D, large-scale manufacturing or in the commercial market. During the R+D phase, most of the costs are attributed to the bioreceptors used in the

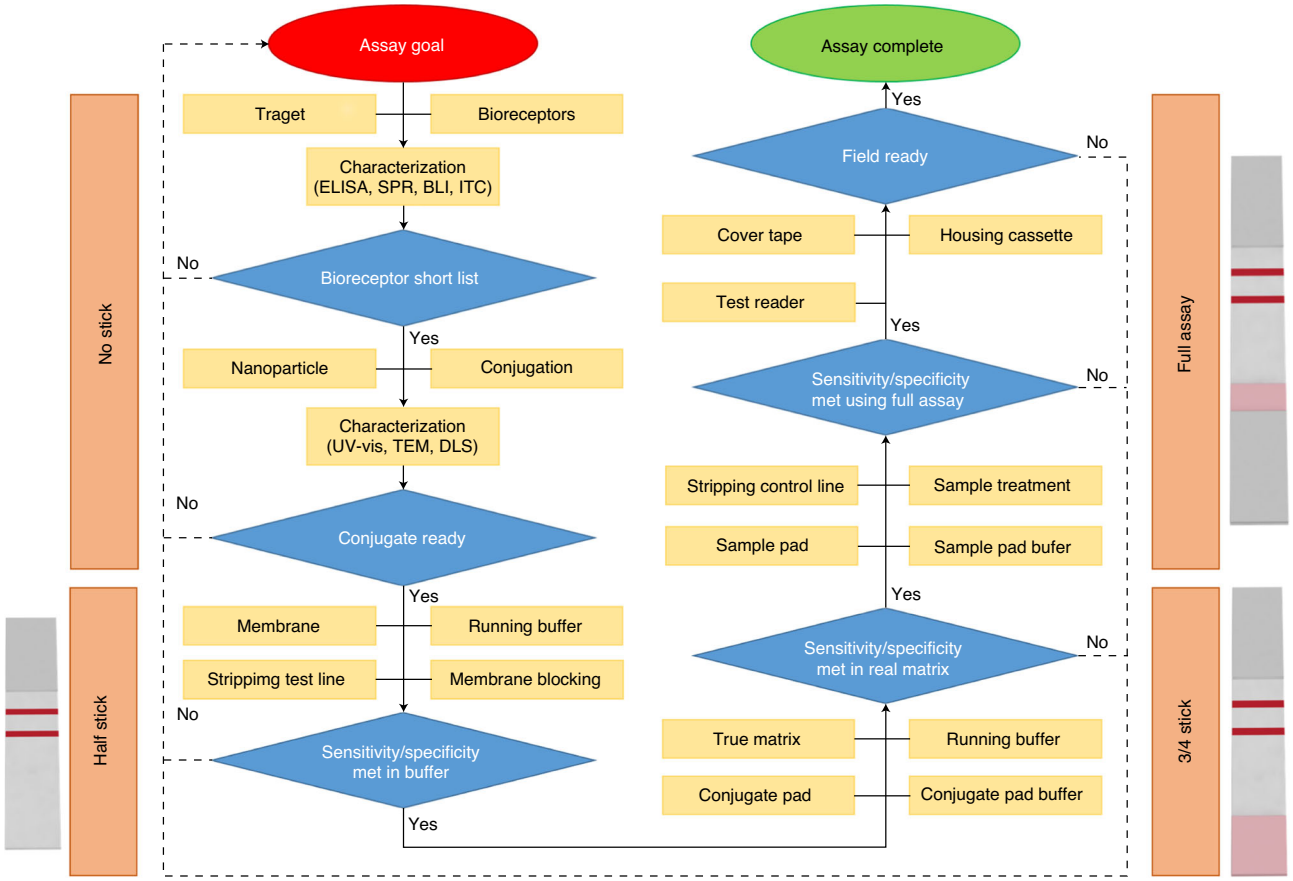

Fig. 8 | Ideal optimization route for the fabrication of an LFA. After setting the assay goal, the developer should short-list the most promising bioreceptors using gold standard techniques (ELISA, SPR, BLI and ITC). The next step is the optimization of the bioreceptor conjugation to the nanoparticle label and the characterization of conjugate stability (using UV-visible light, transmission electron microscopy (TEM) or dynamic light scattering (DLS)). Subsequently, using a half-stick format (just the membrane and absorbent pad), the developer can test several combinations of nanoparticles and bioreceptors to find the most promising ones. During this stage, there is also the first evaluation of the need to block the membrane or not. Then, the developer employs a 3/4 stick format (half stick + conjugate pad) testing the conjugate pad fabrication and the effect of the real sample matrix. During this stage, there is the second evaluation of membrane blocking. If the required sensitivity and specificity are met, then there is the final optimization using the full assay format (3/4 stick plus sample pad and housing cassette). During this phase, the optimization of the sample pad buffer and eventually sample treatment strategies are evaluated before using the housing cassette.

LFA. Generally, we estimate the production costs of a single LF strip to be less than $1 (see Supplementary Table 1 for a detailed example). Despite this low cost, an R+D project for developing a novel LFA could require a lot of financing: labware, consumables, paper, chemical and biological reagents (~$30,000–40,000/year); new equipment and maintenance (~$60,000); laboratory renting, personnel and overcosts (depending on the location, size, employee degree, country, etc.); subcontracting (e.g., materials characterization, regulatory control, legal advice and patentability); and taxes and travel (project meetings, congresses and assay demonstrations). This cost will vary depending on the current status of the facilities, the project and the milestones. The main objective of an R+D phase should be to reach a minimum viable product (MVP), which is an LFA that has demonstrated to have enough repeatability (same response reproduced from the test over time), replicability (same response applying the LFA in different environments) and reproducibility (same response when different operators reconstruct the design) and that clearly differentiates and defines positive and negative responses. Then, with a reliable MVP, the next costs will come from proprietary and regulatory expenses.

In this regard, patentability of a relatively old technology such as LFA can be challenging, as for the patent to be accepted there should be a demonstrable and non-obvious novelty. Generally, the patentability can come from one or more of the following points:

- Biomarker—an LFA detecting a new biomarker, whose presence or absence is related to a specific disease or status.
- Bioreceptor—an LFA using a new bioreceptor for a defined application (e.g., an aptamer sequence).
- Label—an LFA using a new label implying a new detection method, sensing strategy or signal enhancement. However, nanomaterial size modifications, new dyes or conjugation of enzymes on the surface of the label are often not enough to be considered as novel ideas.
- Sensing strategy—an LFA using a new sensing mechanism that leads to a demonstrated advantage over a standard assay. It may include extra steps, reactions or interactions between the different pads, labels and biomarkers.

Box 2 | Example procedure for a lateral flow assay to detect human IgG

This box describes a detailed step-by-step procedure for a traditional sandwich LFA to detect human IgG. In this example, we use two different polyclonal antibodies as capture and detection bioreceptors, the latter one being coupled to gold nanoparticles for qualitative detection by the naked eye and quantitative camera-based detection. Before assembling the LF strip, we provide a detailed procedure to screen for optimal buffers to reduce aggregation of the AuNP-bioreceptor conjugates. Troubleshooting guidance is provided in Table 4.

Materials

Reagents

- *Capture bioreceptor for the test line*. In the example shown in the procedure below, we use an anti-human IgG (whole molecule) antibody produced in goat (Sigma-Aldrich, cat. no. I1886) (RRID: AB_260125)
- *Capture bioreceptor for the control line*. In the example shown in the procedure below, we use a chicken anti-goat IgG H&L (Abcam, cat. no. ab86245) (RRID: AB_1951137). For general recommendations on how to select and validate control line antibodies, see 'Bioreceptor selection' in the main text
- *Detector bioreceptor for conjugation to AuNPs*. In the example shown in the procedure below, we use an anti-human IgG (γ-chain specific) antibody produced in goat (Sigma-Aldrich, cat. no. B1140) (RRID: AB_258513)
- *Target analyte*. In the example shown in the procedure below, we use IgG from human serum (Sigma-Aldrich, cat. no. I2511) (RRID: AB_1163604). See Table 1 and Types of samples and target analytes in the main text for a detailed description of possible target analytes and samples
- BSA (Sigma-Aldrich, cat. no. A3294)
- AuNP solution (gold nanoparticles, 20 nm; BBI Solutions, cat. no. EM.GC20)
- Hydrochloric acid, 37% (wt/wt) (Sigma-Aldrich, cat. no. 320331)
  ! CAUTION Hydrochloric acid may be corrosive to metals, causes severe skin burns and eye damage and may cause respiratory irritation. Do not breathe dust, fumes, gas, mist, vapors or spray. Wear protective gloves, protective clothing, eye protection and face protection. Handle it inside a fume hood.
- NaOH (Sigma-Aldrich, cat. no. S8045)
  ! CAUTION NaOH may be corrosive to metals and can cause severe skin burns and eye damage. Do not breathe dust, fumes, gas, mist, vapors or spray. Wear protective gloves, protective clothing, eye protection and face protection. Handle it inside a fume hood.
- $NaH_2PO_4{\cdot}H_2O$ (Sigma-Aldrich, cat. no. 71504)
- Na_2HPO_4 (Sigma-Aldrich, cat. no. 71640)
- $Na_2B_4O_7{\cdot}10H_2O$ (Sigma-Aldrich, cat. no. B9876)
  ! CAUTION $Na_2B_4O_7{\cdot}10H_2O$ causes serious eye irritation, may damage fertility and may damage an unborn child. Obtain special instructions before use. Do not handle until all safety precautions have been read and understood. Wear protective gloves, protective clothing, eye protection and face protection.
- H_3BO_3 (Sigma-Aldrich, cat. no. B7901)
  ! CAUTION Boric acid may damage fertility and may damage an unborn child. Obtain special instructions before use. If exposed or concerned, get medical advice/attention.
- Sodium citrate ($HOC(COONa)(CH_2COONa)_2{\cdot}2H_2O$; Sigma-Aldrich, cat. no. 1613859)
- Sucrose ($C_{12}H_{22}O_{11}$; Sigma-Aldrich, cat. no. 84097)
- PBS tablets (Sigma-Aldrich, cat. no. P4417)
- Tween-20 (Sigma-Aldrich, cat. no. P1379)
- MilliQ water (produced using the Milli-Q system (>18.2 MΩ · cm))

Equipment

- Detection pad (mdi, cat. no. CNPH200)
- Backing card (Kenosha, cat. no. KN-PS1060.45)
- Sample and absorbent pad (Merck Millipore, cat. no. CFSP001700)
- Conjugate pad (GE Healthcare, Standard 14, cat. no. 8133-2250)
- Graduated pipettes (Gilson P2, 20, 200, 1000)
- Tips for graduated pipettes (Fisherbrand, cat. nos. 10177190 and 10677731)
- Polypropylene graduated microtubes (Eppendorf, cat. no. 0030120248)
- Transfer pipettes (Fisherbrand, cat. no. 13439108)
- Lateral flow assay reader (Skannex, SkanMulti with original equipment manufacturer (OEM) software)
- ThermoShaker for microtubes (Biosan, cat. no. TS-100)
- Centrifuge (Beckman Coulter, Allegra 64R)
- Reagent dispenser (Imagene Technology, IsoFlow reagent dispenser)
- Programmable strip cutter (Kinbio, cat. no. ZQ2002)
- Oven (P. Selecta, cat. no. 2001246)
- Laboratory pump (KNF, Laboport, cat. no. N938.50KN.18)
- Vacuum desiccator (Karnell, cat. no. 550)
- pH meter (Crison, pH meter Basic 20+)
- Analytical balance (Ohaus Discovery; readability: 0.001 g).
- Milli-Q system (>18.2 MΩ · cm) (Millipore)
- Fume hood (Flores Valles)
- Refrigerator and freezer (Premium NoFrost)

Software

- ImageJ version 1.52u (https://imagej.nih.gov/ij/)
- OriginLAb version 8 (https://www.originlab.com/)
- Excel version 2016 (https://products.office.com/en/excel)

Reagent setup

- *PBS (0.01 M; pH 7.4)*. Dissolve one PBS tablet in 200 ml of Milli-Q water. Store it at room temperature (25 °C) for ≤30 d.
- *Phosphate buffer (0.01 M; pH 7.4)*. Dissolve 0.21 g of Na_2HPO_4 in 150 ml of Milli-Q water. Dissolve 0.20 g of $NaH_2PO_4{\cdot}H_2O$ in 150 ml of Milli-Q water. Add a magnetic stirrer, and measure the pH of the Na_2HPO_4 solution under agitation using a pH meter. Add the $NaH_2PO_4{\cdot}H_2O$ solution

Box 2 | Example procedure for a lateral flow assay to detect human IgG (continued)

dropwise to the Na_2HPO_4 solution with a disposable Pasteur pipette until the pH value reaches 7.4. Store it at room temperature for ≤30 d.

- *Borate buffer (10 mM; pH 7).* Dissolve 0.57 g of $Na_2B_4O_7{\cdot}10H_2O$ in 150 ml of Milli-Q water. Dissolve 0.092 g of H_3BO_3 in 150 ml of Milli-Q water. Add a magnetic stirrer, and measure the pH of the $Na_2B_4O_7{\cdot}10H_2O$ solution under agitation using a pH meter. Add the H_3BO_3 solution dropwise to the $Na_2B_4O_7{\cdot}10H_2O$ solution with a disposable Pasteur pipette until the pH value reaches 7. Store it at room temperature for ≤30 d.
- *Borate buffer (100 mM; pH 9).* Dissolve 5.72 g of $Na_2B_4O_7{\cdot}10H_2O$ in 150 ml of Milli-Q water. Dissolve 0.92 g of H_3BO_3 in 150 ml of Milli-Q water. Add a magnetic stirrer, and measure the pH of the $Na_2B_4O_7{\cdot}10H_2O$ solution under agitation using a pH meter. Add the H_3BO_3 solution dropwise to the $Na_2B_4O_7{\cdot}10H_2O$ solution with a disposable Pasteur pipette until the pH value reaches 9. Store it at room temperature for ≤30 d.
- *Conjugate pad buffer.* Prepare a solution of PBS buffer containing 5% (wt/vol) sucrose, 1% (wt/vol) BSA and 0.5% (vol/vol) Tween-20. Store it at 4 °C for ≤7 d.
  ▲ **CRITICAL** The sucrose and Tween-20 in the conjugate pad buffer are imperative for the release and flow of the conjugated AuNP solution along the nitrocellulose strip.
- *Sample pad buffer.* Prepare a solution of PBS buffer containing 0.5% (wt/vol) BSA and 0.05% (vol/vol) Tween-20. Store it at 4 °C for ≤7 d.

Procedure

▲ **CRITICAL** The following simple procedure elucidates the optimal conditions to perform the functionalization of AuNPs with the detection bioreceptor. In particular, it allows the definition of the optimal pH and the minimum antibody concentration to fully cover the nanoparticles. The procedure relies on the propensity of bare (citrate covered using the Turkevic synthesis) gold nanoparticles to aggregate in the presence of high salt concentrations[207,208]. Once the AuNPs are fully covered with the antibody (or with a blocking agent, such as BSA), they remain monodispersed even at high salt concentrations. The aggregation rate can be qualitatively assessed by the naked eye: fully aggregated AuNPs induce a color change in the suspension from red to transparent (due to their precipitation), partially aggregated AuNPs change the color of the suspension from red to blue (due to a shift and widening of their plasmonic peak) and monodispersed AuNPs maintain the original red color[210]. This can be quantitatively measured using UV-visible spectra, DLS, Z-potential and TEM.

Nanoparticle-bioreceptor aggregation test ● Timing 1 h

1 Prepare three solutions of 20-nm diameter AuNPs at pH 7, 8 and 9 (with OD of ~0.450 at 520 nm). Set the correct pH with 10 mM borate buffer (for pH 7) and 100 mM borate buffer (for pH 8 and 9).
2 Prepare dilutions of the detector bioreceptor (detector is anti-human IgG in this example) in Milli-Q water (200, 175, 150, 125, 100, 80, 60, 40 and 0 μg/ml). Prepare a solution of 10% (wt/vol) NaCl in Milli-Q water.
▲ **CRITICAL STEP** Although we typically use a 10% (wt/vol) NaCl solution for the gold aggregation test, it is possible to substitute it with a different buffer (e.g., conjugate pad buffer or LFA running buffer) to study their effects on the stability of the conjugates.
3 In a 96-microwell plate, put 150 μl per well of the AuNP solutions from step 1. Prepare two rows of nine wells for each AuNP solution to create a duplicate test.
4 To each well, add 10 μl of one of the detector antibody dilutions from step 2 in increasing order of antibody concentration (Fig. 3). This will generate final antibody concentrations respectively of 12.5, 10.94, 9.38, 7.81, 6.25, 5.0, 3.75, 2.5 and 0 μg/ml.
▲ **CRITICAL STEP** For easy comparison of the effect of the pH, the wells in each column should have the same antibody concentration.
5 Place the plate on top of the Thermoshaker for 20 min at 600 rpm.
6 Add 20 μl of 10% (wt/vol) NaCl solution to each well.
7 Place the plate back on top of the Thermoshaker for 5 min at 600 rpm.
8 Measure the absorption spectra (from 400 to 600 nm with ≥5 nm between each measurement).
9 From each spectrum, evaluate the peak intensity, peak position and spectra shape (Fig. 3).
▲ **CRITICAL STEP** The maximum absorbance peak of 20-nm-sized AuNPs is at 520 nm. If the AuNPs aggregate in the gold aggregation test, the absorbance peak will shift to the right, and the peak will become wider. The use of the optimal pH and antibody concentration will avoid the aggregation of the AuNPs.
? TROUBLESHOOTING

Large-scale nanoparticle conjugation to the detector bioreceptor ● Timing 1 h 20 min

10 Transfer 1.5 ml of the AuNP solution with the optimal pH (as selected in step 9; in this case, pH 9) in a 2-ml Eppendorf tube.
11 Add the optimized amount of detector antibody in Milli-Q water to the AuNP solution.
▲ **CRITICAL STEP** The starting antibody concentration is defined by the gold aggregation test, but it should be further optimized, generally reducing it. In fact, the gold aggregation test defines the amount of detection bioreceptor that fully covers and thus stabilizes the AuNPs. However, that amount can be reduced (i.e., to reduce the cost of production or to reduce non-specific binding), and the AuNPs can be stabilized with the addition of blocking agents (i.e., BSA). For example, in this case, we are using a final concentration of 2.5 μg/ml detector anti-human IgG, which is lower than the amount defined by the gold aggregation test (6.25 μg/ml, assuming the gold aggregation test value of 100 μg/ml and a molecular weight of 150 kDa), because it provides a lower background signal (Supplementary Fig. 1).
12 Incubate the antibody-AuNP mixture for 20 min at 650 rpm at room temperature using the Thermoshaker.
13 Add 100 μl of 1 mg/ml BSA in Milli-Q water
▲ **CRITICAL STEP** BSA has three functions: it covers any surface area not filled in with the antibody, it helps with stability and it prevents nonspecific adsorption.
14 Incubate the mixture for 20 min at 650 rpm at room temperature using the Thermoshaker.
15 Centrifuge the mixture at 14,000 rpm (30,053*g*) for 20 min at 4 °C.
▲ **CRITICAL STEP** Centrifugation is performed to remove free antibodies that may interfere with the sensitivity of LFA, and multiple centrifugation steps may be required to ensure the complete removal of unbound antibodies. The centrifuge parameters are selected depending on the size of the AuNPs and the volume used. During the centrifugation, the solution tends to heat, and this might affect the stability of the conjugated antibodies. It is therefore recommended to adjust the temperature to 4 °C.
16 Resuspend the antibody-AuNP pellet in 500 μl of the conjugate pad buffer.
▲ **CRITICAL STEP** The dilution factor of the conjugation solution should be carefully selected, as it will affect the dynamic range of the assay. Although a more concentrated solution of AuNPs might provide better detection limits in LFAs, it may affect the flow as well as increase the cost of the sensor.
■ **PAUSE POINT** The antibody-AuNP conjugate can be stored at 4 °C for up to when the antibody or the BSA expires. We recommend verifying the stability of the conjugate before its use, for example, by comparing the UV-visible spectra before and after storage. If there are signs of aggregation (i.e., wider/lower peak compared to the previous measurement), it is recommended to prepare a new conjugate.

Box 2 | Example procedure for a lateral flow assay to detect human IgG (continued)

Lateral flow strip fabrication ● Timing 2 h 30 min

17 *Nitrocellulose membrane striping (steps 17–26).* Fill the reservoirs (test and control line pumps) of the lateral flow dispenser with Milli-Q water and dispense 2,100 µl of Milli-Q water (dispense rate of 5 µl/cm and a speed of 50 mm/s) to clean the syringe, tubing and nozzles.
▲ **CRITICAL STEP** Every lateral flow dispenser has its specific washing procedure. Consult the manual of the specific equipment for details.

18 Empty the supply lines and the reservoirs.

19 Prepare a 200-µl solution of 1 mg/ml capture antibody (capture anti-human IgG in this example) and a 200-µl solution of 1 mg/ml of the control line antibody (anti-goat IgG in this example) in phosphate buffer. Add the control line antibody solution in the reservoir corresponding to the pump for the control line and the capture antibody in the one corresponding to the pump for the test line.
▲ **CRITICAL STEP** The volume of the dispensing solution should be enough to strip the required amount of nitrocellulose membranes. Usually, 100 µl should be enough for the preparation of a 30-cm nitrocellulose membrane using a dispense rate of 0.5 µl/cm and a speed of 50 mm/s in step 22.

20 Prime the pumps and the tubing until a drop flows out of the nozzles.

21 Place the CN200 nitrocellulose membrane (previously attached to the backing card) on the vacuum table.
▲ **CRITICAL STEP** The laminated card side corresponding to the absorbent pad should touch the rear of the table. The position of the nozzles must be manually adjusted to determine the test line and control line positions in the nitrocellulose membrane.

22 Set up the pump system by adjusting the dispense rate to 0.5 µl/cm and the speed to 50 mm/s.
▲ **CRITICAL STEP** Changing the dispense rate and speed will affect the width of the printed lines (Supplementary Fig. 1).

23 Press 'Run' to dispense the capture antibody solution from step 19 onto the test line and the control-line antibody solution onto the control line.
▲ **CRITICAL STEP** Be sure that the dispensed solutions are homogeneous, as this will affect the assay's results. Discard any membrane with faulty lines.

24 Fix the antibodies by drying the detection pad at 37 °C for 2 h in the oven.
? TROUBLESHOOTING

25 *(Optional) Blocking of the membrane with BSA.* To do so, first soak the membrane into the blocking buffer (2% (wt/vol) BSA, 0.01 M PBS, pH 7.4) for 20 min. Next, soak the membrane into the washing buffer (0.05% (wt/vol) SDS, 0.005 M PBS, pH 7.4) with a gentle shake for 15 min. Repeat the washing step at least two times. Finally, dry the membrane at 37 °C for ≥2 h.
▲ **CRITICAL STEP** It is crucial to remove the excess BSA from the membrane; otherwise, it may cover the binding site of the capture and control bioreceptors.

26 Before turning off the lateral flow dispenser, perform a washing procedure with Milli-Q water, followed by 0.1 M HCl, 0.1 M NaOH and again Milli-Q water. Remove the Milli-Q water from the tubing by un-priming the system.
▲ **CRITICAL STEP** Dispense ≥10 syringe volumes during each washing step (dispense rate of 5 µl/cm and a speed of 50 mm/s). The pumps should be thoroughly cleaned monthly using a weak detergent (0.05% sodium C14-16 olefin sulfonate (vol/vol)), 10% (vol/vol) bleach, HCl (0.01 M, pH 2) and NaOH (0.01 M, pH 12).

27 *Sample pad preparation (steps 27 and 28).* Pre-treat the sample pad by dipping it into the sample pad buffer until fully wet.

28 Dry the sample pad at 37 °C for 2 h in the oven.

29 *Conjugation pad preparation (steps 29–39).* Set the dispense rate of the test and control line pumps to 0 µl/mm.

30 Set the air pressure at 0.3–0.6 bar.

31 Fill the spraying pump with Milli-Q water and dispense ≥10 syringe volumes to thoroughly clean the pump.

32 Empty the Milli-Q water of the tube and syringe.

33 Take ≥100 µl of the AuNP-antibody conjugation solution from step 16 and prime it in the spraying syringe.
▲ **CRITICAL STEP** The volume of AuNP-antibody conjugation solution depends on the dispense distance, dispense rate and bed volume of the syringe (step 35).

34 Prime the pumps until a drop of the conjugation solution flows out of the nozzle, and place the conjugate pad on the vacuum table.
▲ **CRITICAL STEP** Place the pad on a clean and thin plastic support plate to avoid the conjugation solution sticking onto the vacuum table.

35 Set up the spraying pump with a dispense rate of 5 µl/mm and a speed of 50 mm/s.

36 Press 'Run' to dispense the conjugation solution onto the conjugate pad.

37 Press 'un-prime' to recycle the conjugation solution.

38 Clean the pumps using Milli-Q water, followed by 0.1 M HCl, Milli-Q water, 0.1 M NaOH and again Milli-Q water. Un-prime the system, and keep the pumps in a liquid-free state.
▲ **CRITICAL STEP** Dispense ≥10 syringe volumes during each washing step (dispense rate of 5 µl/cm and a speed of 50 mm/s). The pumps should be thoroughly cleaned monthly using a weak detergent (0.05% (vol/vol) sodium C14-16 olefin sulfonate), 10% (vol/vol) bleach, HCl (0.01 M, pH 2) and NaOH (0.01 M, pH 12).

39 Dry the conjugate pad in the vacuum chamber for ≥60 min.
▲ **CRITICAL STEP** Check that the conjugate pad is fully dry by evaluating the stiffness of the glass fiber. Check that the AuNP solution is homogeneously distributed throughout the conjugate pad by evaluating the color of the test line by the naked eye.

40 *Assembly of the strips (steps 40 and 41).* Use the plastic guides of the laminated card to assemble the pads accordingly (Fig. 4). After the membrane, place the absorbent pad, then the conjugate pad and finally the sample pad.
? TROUBLESHOOTING

41 Cut the strip at 3 mm width using the strip cutter.
▲ **CRITICAL STEP** In the absence of a dedicated strip cutter, it is possible to cut the strips using a manual guillotine, although the strip-to-strip variability will be higher.
■ **PAUSE POINT** The strips can be stored in a sealed bag with desiccants at 4 °C for as long as the first reagent or material does not expire.

Assay operation and qualitative evaluation ● Timing 1 h

42 Prepare dilutions of the sample containing the target analyte. In this example, we use human IgG in PBS buffer (0, 0.01, 0.03, 0.1. 0.3, 1, 3, 10, 30, 100, 300 and 1,000 ng/ml). For detailed recommendations on the types of samples that can be analyzed, see Types of samples and target analytes in the main text.

43 Drop-cast 70 µl of the sample solution onto the sample pad.
▲ **CRITICAL STEP** The solution should be added dropwise on top of the sample pad to avoid overflow of the sample on top of the conjugate pad and the membrane. This will guarantee that the sample moves along the different pads of the LF strip just by capillarity. In addition, commercial LF strips relying on this type of procedure are often placed in the housing cassette, which limits the possibility of overflow and guarantees the application of the sample always in the same part of the sample pad.

Box 2 | Example procedure for a lateral flow assay to detect human IgG (continued)

▲ **CRITICAL STEP** Alternatively, the strip can be dipped directly into the sample solution, paying attention that just the sample pad is in contact with the sample. This will guarantee that the sample moves along the different pads of the LF strip just by capillarity. While the dropwise method is more convenient from the user perspective (it is more stable and practical), the dipping of the LF strip may be helpful during the development phase (minimizing user variations) or when washing/running buffers are required (after adding the sample, the user would just leave the sample inside a tube containing the desired buffer). In addition, LFAs relying on the dipping method do not require a housing cassette since the LF strip is placed vertically inside the sample.

44 Wait 15 min, and evaluate the strips qualitatively by eye (Fig. 6). Proceed to the next section once the signal in the test and control lines stabilizes.
▲ **CRITICAL STEP** The appearance of signal in the test and control lines indicates the presence of the target analyte (human IgG in this example) in the sample, while the appearance of signal in the control line only indicates the absence of the target analyte in the sample. The signal intensity in the test line correlates with the concentration of the target analyte in the sample. The absence of the control and test lines makes the LFA unreliable and often is indication of a malfunction of the strip.
▲ **CRITICAL STEP** Use a clear and constant white light source, and avoid shadows while evaluating the strips by the naked eye.
? TROUBLESHOOTING

Quantitative evaluation ● **Timing 30 min**

45 Fix the strips in a flat surface under the camera holder (i.e., a tripod or similar).
46 Fix the camera on the camera holder.
47 Adjust the camera parameters, and take pictures of the strips.
▲ **CRITICAL STEP** To facilitate the comparison between different strips and different days it is essential to always use the same set-up, including the distance between the camera and the strips, the light source (ideally in a dark room to prevent contamination from ambient light) and the camera parameters (ISO, aperture, shutter speed and focus).
▲ **CRITICAL STEP** We cannot provide specific indications on the camera parameters to employ, since they may vary from place to place and form camera to camera. Nevertheless, we recommend fixing all the set-up conditions at the beginning of the development and keeping them constant. A simple 'trick' to speed up the optimization of the best camera conditions is to take the first picture using the 'automatic' mode of the camera. Then, use such parameters as a starting point to find the optimal ones.
48 Open the pictures with Image J software (Fig. 7a,b).
49 Select the green channel by selecting Image – Color – Split channel – Green channel (Fig. 7c).
▲ **CRITICAL STEP** The use of the green channel is recommended for the analysis of red labels such as gold nanoparticles since it provides the highest sensitivity.
50 With the 'straight' command, draw a line along the membrane (Fig. 7d).
▲ **CRITICAL STEP** The width of the straight line should be increased until covering most of the strip to obtain more reproducible results.
51 Extract the plot profile by selecting Analyze – Plot profile – List (Fig. 7e).
52 Export the results in data analysis software (Excel, Origin, etc.).
53 Calculate the peak intensity of the test line, and plot it versu the target analyte concentration used (Fig. 7f).
▲ **CRITICAL STEP** the peak intensity can be obtained by subtracting the peak value of the test line from the background value. Overall, it is not recommended to use the peak value of the control line as a reference for the test line one, since high target analyte concentrations (in a sandwich assay) may lead to a dramatic depletion in the concentration of AuNPs after the test line, which may produce a decrease in the control line intensity (if compared to strips that used low target concentrations).
54 Fit the data to a four-parameter logistic curve (sigmoidal curve)[209].
▲ **CRITICAL STEP** In the case of using a range of target concentrations that generates both non-responsive and saturated signals, the best data fitting is generally obtained using a four-parameter logisitic curve (a sigmoidal curve). However, if the calibration is done using a range of target concentrations focused on the dynamic range of the fitted sigmoidal curve (between 10% and 90% of the maximum signal), it is possible to approximate the fit to a linear curve. Generally, sigmoidal approximation is accepted for competitive immunoassays (since they more closely represent an ideal Langmuir model than an immune sandwich assay), whereas linear approximation of the initial part of concentration dependence is often preferred for immune sandwich assays.
55 Carry out the desired statistical analysis such as calculating the LoD and the LoQ.
▲ **CRITICAL STEP** It is possible to calculate the LoD (value of the blank + three times its standard deviation) and LoQ (value of the blank + 10 times its standard deviation), which in this case is 0.77 and 4.62 nM, respectively. As shown also by this example dataset (where the LoD signal is almost undistinguishable from the non-responsive portion of the fitted curve), although LoD is a generally accepted method to evaluate LFAs, it is sometimes not statistically robust since it does not count for the variance in the test signals. We refer the reader to the following references describing improved methods to calculate the LoD of LFAs[186,210–212].
? TROUBLESHOOTING

- New materials—an LFA using new materials as pads or membrane; however, size modifications on the pads and parameters, such as porosity and protein affinity, are difficult to protect.
- New design—an LFA that employs a new functionality or has an identifiable trademark.

Patenting processes are long (more than one year in most cases), and the costs are generally high (evaluation and certifying costs), leading also to maintenance costs. The patent cost will also vary depending on the level of protection of the technology (country wide, continent wide or worldwide). In addition to the requirements of each country in which the LFA will be used, regulation and approval (see next section) expenses will also depend on the target user and environment. During this phase, the R+D laboratory will still be in charge of producing and providing the product for its evaluation.

After R+D, with the MVP protected and approved for the market, the next phase is mass production. During mass production in a factory, the cost per LF strip decreases to ~$0.01, although this does not include equipment and their maintenance, the employees, insurance, taxes, quality control and many other indirect costs. Finally, the market cost is the toughest one to estimate. For the sake of comparison, we will use the cost of 'Clearblue Rapid Detection Pregnancy Test', which we can purchase for ~$6 per test. Although it could seem that there is a great benefit for the company and the seller, there are also even more indirect costs such as packaging (cassettes, bags, desiccants, etc.) and storage of the product, shipping,

Table 4 | Troubleshooting table

Step	Problem	Possible reason	Solution
	The target analyte is not commercially available The target analyte is too expensive	The target analyte is new or not common	Produce your own target analyte Purify the target analyte from real samples
	Bioreceptors are not commercially available Bioreceptors are too expensive	The target analyte is new or not common	Evaluate different types of bioreceptors (Table 3) Develop new bioreceptors Consider changing the assay format from sandwich to competitive assay
	Bioreceptors are not sensitive and specific enough, as determined using standard techniques (ELISA, SPR, etc.)	The target analyte is new or not common The target analyte concentration is too low	Develop new bioreceptors Consider whether sample treatment, target pre-concentration or signal amplification could solve the issue Re-evaluate your assay's goals
9	Nanoparticles are not stable in solution after conjugation with the bioreceptor	The ionic strength of the buffer is too high The conjugation was not successful	Decrease buffer ionic strength or increase amount of surfactants or BSA Increase the amount of bioreceptor during the conjugation Increase the amount of bioreceptor during the conjugation Block the nanoparticles with stabilizing agents (i.e., BSA) Evaluate different conjugation strategies
44	Nanoparticles do not flow upon rewetting	Nanoparticles are stuck on the conjugate pad	Increase the sugar concentration in the conjugate pad buffer Verify that the conjugate pad is fully dried before adding the sample Increase the amount of surfactant in the running buffer If using polyclonal antibodies, control for the formation of immune aggregates Change the conjugate pad material Re-optimize conjugation
	Sample does not reach the conjugate pad	The sample pad is clogged The sample pad and the conjugate pad are not in contact	Use a different sample pad material Introduce an extra filtration or sample treatment to remove bigger particles Use an extra running or washing buffer Ensure that the sample and conjugate pad are overlaid Ensure that the sample pad is not compressed by the cassette Change composition of the sample pad buffer, increasing the amount of surfactant
	The test line does not show up, but the control line does	The target concentration is too low or too high The test line bioreceptor was not properly striped If using a sandwich assay, the bioreceptors bind the same epitope	Check a wider range of target concentrations (sandwich assay can also present the hook effect[205]) Decrease the ionic strength of the striping buffer Remove/decrease surfactants from striping and running buffers Increase the concentration of the bioreceptor or add other molecules (BSA) to stabilize it Remove membrane blocking (if any), or decrease the blocking agent concentration Increase the amount of the label in the conjugate pad Ensure that the bioreceptor is completely dried before using the LFA Change the bioreceptor
	The control line does not show up, but the test line does	The control line bioreceptor was not properly striped The bioreceptor-nanoparticle conjugate concentration is too low	Add a different nanoparticle specific for the control line Decrease the ionic strength of the striping buffer Remove surfactants from the striping buffer Increase the amount of nanoparticles in the conjugate pad Change to a different capture bioreceptor

Table continued

Table 4 (continued)

Step	Problem	Possible reason	Solution
24	The sensor is not specific	Nonspecific interactions induce the accumulation of label on the test line even in the absence of target	Change to different bioreceptors Block the membrane Increase blocking agents in the sample pad and running buffers Increase the amount of surfactants in the striping, sample pad and running buffers Increase the ionic strength in the sample pad and running buffers Change pH in the sample pad and running buffers Use a faster flow membrane Actively remove possible contaminants
	Both the control and test lines do not show up	The bioreceptor-nanoparticle conjugation was not successful The striping was wrong The target concentration is too high	Change conjugation strategy Change the striping buffer, decrease ionic strength and remove surfactants Decrease the surfactant concentration in the running buffer Use a new membrane (in case it is expired) or change material Verify that the capture bioreceptors are actually striped on the membrane Verify that the labeled bioreceptor is not expired Dilute the sample
44	The cutoff value is not adequate for the application (i.e., the sensor is too sensitive or not sensitive enough to detect the target concentration of interest)	The sensor cannot detect application-relevant concentrations of the target	Increase the amount of nanoparticles Use a slower flow membrane Change the amount of bioreceptors on the test line Change the ionic strength, pH and surfactant concentration in the buffers Change the type of nanoparticles and sensing strategy Pre-concentrate or dilute the sample depending on what is appropriate Include a signal amplification step Change to different bioreceptors
44–55	The sensitivity is not adequate for the application	The sensor cannot accurately differentiate two close concentration values	Increase the amount of nanoparticles Use a slower flow membrane Change the amount of bioreceptors on the test line Change the ionic strength, pH and surfactant concentration in the buffers Change the type of nanoparticles and the sensing strategy Pre-concentrate the sample Apply a signal amplification strategy Change to different bioreceptors Modify the strip dimensions and architecture Consider pre-treatment of the sample (purification, amplification, not dilution, etc.) and/or increase the sample volume Improve the quantification device (camera, sensor, software, etc.)
	The sensor does not show repeatability	Using the same target concentration, the sensor produces different signals	Verify the fabrication steps and that the ambient conditions are constant from batch to batch Use a constant light source If using a reader, use the same parameters (i.e., exposure, focus, etc.) Ensure the proper storage of the LFA
	The sensor is not reproducible	Other developers or users do not obtain the same response[206]	Verify the fabrication steps and that the ambient conditions are constant from batch to batch Use a constant light source Define protocols to store all the reagents involved and control parameters such as pH during all the steps Evaluate incubation steps at different times/temperatures Define expiration dates for reagents, materials and the device itself Provide a more precise and easier-to-understand protocol to facilitate sensor operation by the user

marketing, taxes, additional reagents and tools and the cost of R+D and clinical validation that need to be taken into account.

Regulation and approval

An LFA for the purpose of PoC, or clinical environments, is considered a medical device, and its use is regulated by governmental institutions, such as the European Medicines Agency in the European Union (EU) and the Food and Drug Administration in the United States. In the EU, medical devices have to undergo a conformity assessment to demonstrate that the legal requirements are met to ensure that they are safe. Accredited national authorities are responsible for conducting these conformity assessments that, once fulfilled, award the device the CE ('Conformité Européenne'; translation: European Conformity) mark.

Furthermore, LFAs also work as in vitro assays, meaning that the device does not affect the organism being tested. In this case, after obtaining the MVP and to obtain the CE mark (or the regional corresponding indicator), the device should be validated as indicated by the relevant institution. Depending on the origin of the samples, an ethical committee may have to evaluate the process.

Future directions

LFAs have been some of the most popular biosensors for the past decades, and we believe they still have a bright future ahead, especially if developers will design them to address the challenges that personalized/precision medicine and in-the-field environmental analysis will present. Regarding clinical purposes, we believe there are two major goals that the next generation of LFAs should tackle: (i) the sensitive and quantitative detection of multiple protein targets at under pM concentrations[3,178–182] (e.g., using a microarray-type approach)[187] and (ii) the integration into a single LFA strip of both a nucleic acid amplification and detection[188–194]. Similarly, for environmental analysis, an improvement in the sensitivity and quantitative measuring of multiple targets will be required, together with the development of LFAs detecting families of compounds rather than specific molecules. Succeeding in these tasks will require a joint effort between different disciplines, ranging from the selection of bioreceptors showing desirable characteristics for LFAs (fast binding kinetics and stability), to the development of novel materials showing superior properties (either labels or new membranes, pads and filters[195]), to the use of programming to optimize the fabrication of LFAs and their quantitative analysis using portable readers.

Reporting Summary

Further information on research design is available in the Nature Research Reporting Summary linked to this article.

Data availability

The datasets generated during and/or analyzed during the current study (Figs. 3 and 7) are available from the corresponding author on reasonable request.

References

1. Parolo, C. & Merkoçi, A. Paper-based nanobiosensors for diagnostics. *Chem. Soc. Rev.* **42**, 450–457 (2013).
2. Bahadır, E. B. & Sezgintürk, M. K. Lateral flow assays: principles, designs and labels. *Trends Analyt. Chem.* **82**, 286–306 (2016).
3. Brangel, P. et al. A serological point-of-care test for the detection of IgG antibodies against Ebola virus in human survivors. *ACS Nano* **12**, 63–73 (2018).
4. Posthuma-Trumpie, G. A., Korf, J. & van Amerongen, A. Lateral flow (immuno)assay: its strengths, weaknesses, opportunities and threats. A literature survey. *Anal. Bioanal. Chem.* **393**, 569–582 (2009).
5. Hu, J. et al. Advances in paper-based point-of-care diagnostics. *Biosens. Bioelectron.* **54**, 585–597 (2014).
6. Yetisen, A. K., Akram, M. S. & Lowe, C. R. Paper-based microfluidic point-of-care diagnostic devices. *Lab Chip* **13**, 2210–2251 (2013).
7. Martinelli, F. et al. Advanced methods of plant disease detection. A review. *Agron. Sustain. Dev* **35**, 1–25 (2015).
8. Li, P., Zhang, Q. & Zhang, W. Immunoassays for aflatoxins. *Trends Analyt. Chem.* **28**, 1115–1126 (2009).
9. Anfossi, L., Baggiani, C., Giovannoli, C., D'Arco, G. & Giraudi, G. Lateral-flow immunoassays for mycotoxins and phycotoxins: a review. *Anal. Bioanal. Chem.* **405**, 467–480 (2013).
10. Luo, K., Kim, H.-Y., Oh, M.-H. & Kim, Y.-R. Paper-based lateral flow strip assay for the detection of foodborne pathogens: principles, applications, technological challenges and opportunities. *Crit. Rev. Food Sci. Nutr.* **60**, 157–170 (2020).
11. Ahmed, F. E. Detection of genetically modified organisms in foods. *Trends Biotechnol.* **20**, 215–223 (2002).
12. Ngom, B., Guo, Y., Wang, X. & Bi, D. Development and application of lateral flow test strip technology for detection of infectious agents and chemical contaminants: a review. *Anal. Bioanal. Chem.* **397**, 1113–1135 (2010).
13. Zhao, X., Lin, C.-W., Wang, J. & Oh, D. H. Advances in rapid detection methods for foodborne pathogens. *J. Microbiol. Biotechnol.* **24**, 297–312 (2014).
14. Ramage, J. G. et al. Comprehensive laboratory evaluation of a specific lateral flow assay for the presumptive identification of abrin in suspicious white powders and environmental samples. *Biosecur. Bioterror.* **12**, 49–62 (2014).
15. Grubb, A. O. & Glad, U. C. Immunoassay with test strip having antibodies bound thereto. US Patent 4,168,146 filed 15 January 1976 and issued 18 September 1979.
16. Hsieh, H. V., Dantzler, J. L. & Weigl, B. H. Analytical tools to improve optimization procedures for lateral flow assays. *Diagnostics* **7**, 29 (2017).
17. Gasperino, D., Baughman, T., Hsieh, H. V., Bell, D. & Weigl, B. H. Improving lateral flow assay performance using computational modeling. *Annu. Rev. Anal. Chem.* **11**, 219–244 (2018).
18. Merck Millipore. Rapid lateral flow test strips: considerations for product development. http://www.merckmillipore.com/INTERSHOP/web/WFS/Merck-RU-Site/ru_RU/-/USD/ShowDocument-Pronet?id=201306.15671 (2013; accessed 28 July 2020).
19. nanoComposix. Lateral flow assay development guide. https://nanocomposix.com/pages/lateral-flow-assay-development-guide (2018; accessed 28 July 2020).
20. Wong, R. C. & Tse, H. Y., eds. *Lateral Flow Immunoassay* (Humana Press, 2009).
21. Bishop, J. D., Hsieh, H. V., Gasperino, D. J. & Weigl, B. H. Sensitivity enhancement in lateral flow assays: a systems perspective. *Lab Chip* **19**, 2486–2499 (2019).
22. Zhang, G., Guo, J. & Wang, X. Immunochromatographic lateral flow strip tests. In *Biosensors and Biodetection. Methods in*

Molecular Biology (eds. Rasooly, A. & Herold, K. E.) 169–183 (Humana Press, 2009).
23. Volkov, A., Mauk, M., Corstjens, P. & Niedbala, R. S. Rapid prototyping of lateral flow assays. In *Biosensors and Biodetection. Methods in Molecular Biology* (eds. Rasooly, A. & Herold, K. E.) 217–235 (Humana Press, 2009).
24. Bailes, J., Mayoss, S., Teale, P. & Soloviev, M. Gold nanoparticle antibody conjugates for use in competitive lateral flow assays. In *Nanoparticles in Biology and Medicine. Methods in Molecular Biology (Methods and Protocols)* Vol. 906 (ed. Soloviev, M.) 45–55 (Humana Press, 2012).
25. Zeng, L., Lie, P., Fang, Z. & Xiao, Z. Lateral flow biosensors for the detection of nucleic acid. In *Nucleic Acid Detection. Methods in Molecular Biology (Methods and Protocols)* Vol. **1039** (eds. Kolpashchikov, D. & Gerasimova, Y.) 161–167 (Humana Press, 2013).
26. Ching, K. H. Lateral flow immunoassay. in *ELISA: Methods in Molecular Biology* (ed. Hnasko, R.) 127–137 (Humana Press, 2015).
27. Tang, R. H. et al. Advances in paper-based sample pretreatment for point-of-care testing. *Crit. Rev. Biotechnol.* **37**, 411–428 (2017).
28. Wang, Y. et al. A SERS-based lateral flow assay biosensor for quantitative and ultrasensitive detection of interleukin-6 in unprocessed whole blood. *Biosens. Bioelectron.* **141**, 111432 (2019).
29. Ang, S. H., Rambeli, M., Thevarajah, T. M., Alias, Y. B. & Khor, S. M. Quantitative, single-step dual measurement of hemoglobin A1c and total hemoglobin in human whole blood using a gold sandwich immunochromatographic assay for personalized medicine. *Biosens. Bioelectron.* **78**, 187–193 (2016).
30. Gao, X. et al. Paper-based surface-enhanced raman scattering lateral flow strip for detection of neuron-specific enolase in blood plasma. *Anal. Chem.* **89**, 10104–10110 (2017).
31. Dieplinger, B., Egger, M., Gegenhuber, A., Haltmayer, M. & Mueller, T. Analytical and clinical evaluation of a rapid quantitative lateral flow immunoassay for measurement of soluble ST2 in human plasma. *Clin. Chim. Acta* **451**, 310–315 (2015).
32. Ou, L. et al. Development of a lateral flow immunochromatographic assay for rapid detection of *Mycoplasma pneumoniae*-specific IgM in human serum specimens. *J. Microbiol. Methods* **124**, 35–40 (2016).
33. Huang, Y. et al. Development of up-converting phosphor technology-based lateral flow assay for quantitative detection of serum PIVKA-II: inception of a near-patient PIVKA-II detection tool. *Clin. Chim. Acta* **488**, 202–208 (2019).
34. Chamorro-Garcia, A. et al. Detection of parathyroid hormone-like hormone in cancer cell cultures by gold nanoparticle-based lateral flow immunoassays. *Nanomedicine* **12**, 53–61 (2016).
35. Dalirirad, S. & Steckl, A. J. Aptamer-based lateral flow assay for point of care cortisol detection in sweat. *Sens. Actuators B Chem.* **283**, 79–86 (2019).
36. Hudson, M. et al. Drug screening using the sweat of a fingerprint: lateral flow detection of Δ9-tetrahydrocannabinol, cocaine, opiates and amphetamine. *J. Anal. Toxicol.* **43**, 88–95 (2019).
37. Dalirirad, S. & Steckl, A. J. Lateral flow assay using aptamer-based sensing for on-site detection of dopamine in urine. *Anal. Biochem.* **596**, 113637 (2020).
38. Li, Z., Chen, H., Feng, S., Liu, K. & Wang, P. Development and clinical validation of a sensitive lateral flow assay for rapid urine fentanyl screening in the emergency department. *Clin. Chem.* **66**, 324–332 (2020).
39. Henderson, W. A. et al. Simple lateral flow assays for microbial detection in stool. *Anal. Methods* **10**, 5358–5363 (2018).
40. Lin, Z. et al. Development of an immunochromatographic lateral flow device for rapid detection of *Helicobacter pylori* stool antigen. *Clin. Biochem.* **48**, 1298–1303 (2015).
41. Hu, Q. et al. An up-converting phosphor technology-based lateral flow assay for point-of-collection detection of morphine and methamphetamine in saliva. *Analyst* **143**, 4646–4654 (2018).
42. Oh, H.-K., Kim, J.-W., Kim, J.-M. & Kim, M.-G. High sensitive and broad-range detection of cortisol in human saliva using a trap lateral flow immunoassay (trapLFI) sensor. *Analyst* **143**, 3883–3889 (2018).
43. Boulware, D. R. et al. Multisite validation of cryptococcal antigen lateral flow assay and quantification by laser thermal contrast. *Emerg. Infect. Dis.* **20**, 45–53 (2014).
44. Fleury, A. et al. A lateral flow assay (LFA) for the rapid detection of extraparenchymal neurocysticercosis using cerebrospinal fluid. *Exp. Parasitol.* **171**, 67–70 (2016).
45. Sakurai, A. et al. Multi-colored immunochromatography using nanobeads for rapid and sensitive typing of seasonal influenza viruses. *J. Virol. Methods* **209**, 62–68 (2014).
46. Eryılmaz, M. et al. SERS-based rapid assay for sensitive detection of Group A *Streptococcus* by evaluation of the swab sampling technique. *Analyst* **144**, 3573–3580 (2019).
47. Principato, M. et al. Detection of target staphylococcal enterotoxin B antigen in orange juice and popular carbonated beverages using antibody-dependent antigen-capture assays. *J. Food Sci.* **75**, T141–T147 (2010).
48. Jiang, H. et al. Silver nanoparticle-based fluorescence-quenching lateral flow immunoassay for sensitive detection of ochratoxin A in grape juice and wine. *Toxins (Basel)* **9**, 83 (2017).
49. Kong, D. et al. Ultrasensitive and eco-friendly immunoassays based monoclonal antibody for detection of deoxynivalenol in cereal and feed samples. *Food Chem.* **270**, 130–137 (2019).
50. Focker, M., van der Fels-Klerx, H. J. & Oude Lansink, A. G. J. M. Cost-effective sampling and analysis for mycotoxins in a cereal batch. *Risk Anal.* **39**, 926–939 (2019).
51. Yang, X. et al. A lateral flow immunochromato-graphic strip test for rapid detection of oseltamivir phosphate in egg and chicken meat. *Sci. Rep.* **8**, 16680 (2018).
52. Magiati, M., Myridaki, V. M., Christopoulos, T. K. & Kalogianni, D. P. Lateral flow test for meat authentication with visual detection. *Food Chem.* **274**, 803–807 (2019).
53. Tan, G. et al. Ultrasensitive quantitation of imidacloprid in vegetables by colloidal gold and time-resolved fluorescent nanobead traced lateral flow immunoassays. *Food Chem.* **311**, 126055 (2020).
54. Hassan, A. H. A., Bergua, J. F., Morales-Narváez, E. & Mekoçi, A. Validity of a single antibody-based lateral flow immunoassay depending on graphene oxide for highly sensitive determination of *E. coli* O157:H7 in minced beef and river water. *Food Chem.* **297**, 124965 (2019).
55. Liu, Y. et al. Detection of 3-phenoxybenzoic acid in river water with a colloidal gold-based lateral flow immunoassay. *Anal. Biochem.* **483**, 7–11 (2015).
56. Wu, Z. et al. Aptamer-based fluorescence-quenching lateral flow strip for rapid detection of mercury (II) ion in water samples. *Anal. Bioanal. Chem.* **409**, 5209–5216 (2017).
57. Quesada-González, D., Jairo, G. A., Blake, R. C., Blake, D. A. & Merkoçi, A. Uranium (VI) detection in groundwater using a gold nanoparticle/paper-based lateral flow device. *Sci. Rep* **8**, 16157 (2018).
58. Mosley, G. L. et al. Improved lateral-flow immunoassays for chlamydia and immunoglobulin M by sequential rehydration of two-phase system components within a paper-based diagnostic. *Microchim. Acta* **184**, 4055–4064 (2017).

59. Ridgway, K., Lalljie, S. P. D. & Smith, R. M. Sample preparation techniques for the determination of trace residues and contaminants in foods. *J. Chromatogr. A* **1153**, 36–53 (2007).
60. Gong, M. M., Macdonald, B. D., Vu Nguyen, T., Van Nguyen, K. & Sinton, D. Field tested milliliter-scale blood filtration device for point-of-care applications. *Biomicrofluidics* **7**, 44111 (2013).
61. Golden, A. et al. Extended result reading window in lateral flow tests detecting exposure to *Onchocerca volvulus*: a new technology to improve epidemiological surveillance tools. *PLoS ONE* **8**, e69231 (2013).
62. Sastre, P. et al. Development of a novel lateral flow assay for detection of African swine fever in blood. *BMC Vet. Res.* **12**, 206 (2016).
63. Choi, J. R. et al. Sensitive biomolecule detection in lateral flow assay with a portable temperature–humidity control device. *Biosens. Bioelectron.* **79**, 98–107 (2016).
64. Fukushi, S. et al. Characterization of novel monoclonal antibodies against the MERS-coronavirus spike protein and their application in species-independent antibody detection by competitive ELISA. *J. Virol. Methods* **251**, 22–29 (2018).
65. Duo, J. et al. Surface plasmon resonance as a tool for ligand-binding assay reagent characterization in bioanalysis of biotherapeutics. *Bioanalysis* **10**, 559–576 (2018).
66. Miller, B. S. et al. Quantifying biomolecular binding constants using video paper analytical devices. *Chemistry* **24**, 9783–9787 (2018).
67. Dam, T. K., Torres, M., Brewer, C. F. & Casadevall, A. Isothermal titration calorimetry reveals differential binding thermodynamics of variable region-identical antibodies differing in constant region for a univalent ligand. *J. Biol. Chem.* **283**, 31366–31370 (2008).
68. Yang, D., Singh, A., Wu, H. & Kroe-Barrett, R. Determination of high-affinity antibody-antigen binding kinetics using four biosensor platforms. *J. Vis. Exp.* e55659 (2017).
69. Mosley, G. L., Nguyen, P., Wu, B. M. & Kamei, D. T. Development of quantitative radioactive methodologies on paper to determine important lateral-flow immunoassay parameters. *Lab Chip* **16**, 2871–2881 (2016).
70. Wang, C. et al. Lateral flow immunoassay integrated with competitive and sandwich models for the detection of aflatoxin M1 and *Escherichia coli* O157:H7 in milk. *J. Dairy Sci.* **101**, 8767–8777 (2018).
71. Nguyen, V.-T., Song, S., Park, S. & Joo, C. Recent advances in high-sensitivity detection methods for paper-based lateral-flow assay. *Biosens. Bioelectron.* **152**, 112015 (2020).
72. Quesada-González, D. & Merkoçi, A. Nanoparticle-based lateral flow biosensors. *Biosens. Bioelectron.* **73**, 47–63 (2015).
73. Soh, J. H., Chan, H.-M. & Ying, J. Y. Strategies for developing sensitive and specific nanoparticle-based lateral flow assays as point-of-care diagnostic device. *Nano Today* **30**, 100831 (2020).
74. Ge, X. et al. Nanomaterial-enhanced paper-based biosensors. *Trends Analyt. Chem.* **58**, 31–39 (2014).
75. Zhan, L. et al. The role of nanoparticle design in determining analytical performance of lateral flow immunoassays. *Nano Lett.* **17**, 7207–7212 (2017).
76. Quesada-González, D. & Merkoçi, A. Nanomaterial-based devices for point-of-care diagnostic applications. *Chem. Soc. Rev.* **47**, 4697–4709 (2018).
77. Verheijen, R., Osswald, I. K., Dietrich, R. & Haasnoot, W. Development of a one step strip test for the detection of (dihydro) streptomycin residues in raw milk. *Food Agric. Immunol.* **12**, 31–40 (2000).
78. Fong, W. K. et al. Rapid solid-phase immunoassay for detection of methicillin-resistant *Staphylococcus aureus* using cycling probe technology. *J. Clin. Microbiol* **38**, 2525–2529 (2000).
79. Shyu, R. H., Shyu, H. F., Liu, H. W. & Tang, S. S. Colloidal gold-based immunochromatographic assay for detection of ricin. *Toxicon* **40**, 255–258 (2002).
80. Ren, W., Ballou, D. R., FitzGerald, R. & Irudayaraj, J. Plasmonic enhancement in lateral flow sensors for improved sensing of *E. coli* O157:H7. *Biosens. Bioelectron.* **126**, 324–331 (2019).
81. Innova Biosciences. Guide to lateral flow immunoassays: Innova Biosciences guide. https://fnkprddata.blob.core.windows.net/domestic/download/pdf/IBS_A_guide_to_lateral_flow_immunoassays.pdf (2020; accessed 28 July 2020).
82. Di Nardo, F., Cavalera, S., Baggiani, C., Giovannoli, C. & Anfossi, L. Direct vs mediated coupling of antibodies to gold nanoparticles: the case of salivary cortisol detection by lateral flow immunoassay. *ACS Appl. Mater. Interfaces* **11**, 32758–32768 (2019).
83. Parolo, C. et al. Design, preparation, and evaluation of a fixed-orientation antibody/gold-nanoparticle conjugate as an immunosensing label. *ACS Appl. Mater. Interfaces* **5**, 10753–10759 (2013).
84. Liu, J., Mazumdar, D. & Lu, Y. A simple and sensitive 'dipstick' test in serum based on lateral flow separation of aptamer-linked nanostructures. *Angew. Chem. Int. Ed. Engl.* **45**, 7955–7959 (2006).
85. Mao, X. et al. Disposable nucleic acid biosensors based on gold nanoparticle probes and lateral flow strip. *Anal. Chem.* **81**, 1660–1668 (2009).
86. Posthuma-Trumpie, G. A., Wichers, J. H., Koets, M., Berendsen, L. B. J. M. & van Amerongen, A. Amorphous carbon nanoparticles: a versatile label for rapid diagnostic (immuno)assays. *Anal. Bioanal. Chem.* **402**, 593–600 (2012).
87. Van Dam, G. J. et al. Diagnosis of schistosomiasis by reagent strip test for detection of circulating cathodic antigen. *J. Clin. Microbiol.* **42**, 5458–5461 (2004).
88. Blazková, M., Micková-Holubová, B., Rauch, P. & Fukal, L. Immunochromatographic colloidal carbon-based assay for detection of methiocarb in surface water. *Biosens. Bioelectron.* **25**, 753–758 (2009).
89. Blažková, M., Rauch, P. & Fukal, L. Strip-based immunoassay for rapid detection of thiabendazole. *Biosens. Bioelectron.* **25**, 2122–2128 (2010).
90. Kalogianni, D. P., Boutsika, L. M., Kouremenou, P. G., Christopoulos, T. K. & Ioannou, P. C. Carbon nano-strings as reporters in lateral flow devices for DNA sensing by hybridization. *Anal. Bioanal. Chem.* **400**, 1145–1152 (2011).
91. Noguera, P. et al. Carbon nanoparticles in lateral flow methods to detect genes encoding virulence factors of Shiga toxin-producing *Escherichia coli*. *Anal. Bioanal. Chem.* **399**, 831–838 (2011).
92. Oliveira-Rodríguez, M. et al. Point-of-care detection of extracellular vesicles: sensitivity optimization and multiple-target detection. *Biosens. Bioelectron.* **87**, 38–45 (2017).
93. Qiu, W. et al. Carbon nanotube-based lateral flow biosensor for sensitive and rapid detection of DNA sequence. *Biosens. Bioelectron.* **64**, 367–372 (2015).
94. Yao, L. et al. MWCNTs based high sensitive lateral flow strip biosensor for rapid determination of aqueous mercury ions. *Biosens. Bioelectron.* **85**, 331–336 (2016).
95. Greenwald, R. et al. Improved serodetection of *Mycobacterium bovis* infection in badgers (*Meles meles*) using multiantigen test formats. *Diagn. Microbiol. Infect. Dis.* **46**, 197–203 (2003).
96. Morales-Narváez, E., Naghdi, T., Zor, E. & Merkoçi, A. Photoluminescent lateral-flow immunoassay revealed by graphene oxide: highly sensitive paper-based pathogen detection. *Anal. Chem.* **87**, 8573–8577 (2015).
97. Medintz, I. L., Uyeda, T. H., Goldman, E. R. & Mattoussi, H. Quantum dot bioconjugates for imaging, labelling and sensing. *Nat. Mater.* **4**, 435–446 (2005).

98. Taranova, N. A., Berlina, A. N., Zherdev, A. V. & Dzantiev, B. B. 'Traffic light' immunochromatographic test based on multicolor quantum dots for the simultaneous detection of several antibiotics in milk. *Biosens. Bioelectron.* **63**, 255–261 (2015).
99. Foubert, A. et al. Development of a rainbow lateral flow immunoassay for the simultaneous detection of four mycotoxins. *J. Agric. Food Chem.* **65**, 7121–7130 (2017).
100. Wang, C. et al. Layer-by-layer assembly of magnetic-core dual quantum dot-shell nanocomposites for fluorescence lateral flow detection of bacteria. *Nanoscale* **12**, 795–807 (2020).
101. Yan, X. et al. CdSe/ZnS quantum dot-labeled lateral flow strips for rapid and quantitative detection of gastric cancer carbohydrate antigen 72-4. *Nanoscale Res. Lett.* **11**, 138 (2016).
102. Berlina, A. N., Taranova, N. A., Zherdev, A. V., Vengerov, Y. Y. & Dzantiev, B. B. Quantum dot-based lateral flow immunoassay for detection of chloramphenicol in milk. *Anal. Bioanal. Chem.* **405**, 4997–5000 (2013).
103. Bruno, J. G. Application of DNA aptamers and quantum dots to lateral flow test strips for detection of foodborne pathogens with improved sensitivity versus colloidal gold. *Pathogens* **3**, 341–355 (2014).
104. Bruno, J. G. Evaluation of pathogenic big 7 *E. coli* aptamer-quantum dot lateral flow test strips. *J. Bionanoscience* **11**, 148–152 (2017).
105. Yang, H. et al. A novel quantum dots-based point of care test for syphilis. *Nanoscale Res. Lett.* **5**, 875–881 (2010).
106. Zamora-Gálvez, A., Morales-Narváez, E., Romero, J. & Merkoçi, A. Photoluminescent lateral flow based on non-radiative energy transfer for protein detection in human serum. *Biosens. Bioelectron.* **100**, 208–213 (2018).
107. Chen, J. et al. A facile fluorescence lateral flow biosensor for glutathione detection based on quantum dots-MnO2 nanocomposites. *Sens. Actuators B Chem.* **260**, 770–777 (2018).
108. Rong, Z. et al. Dual-color magnetic-quantum dot nanobeads as versatile fluorescent probes in test strip for simultaneous point-of-care detection of free and complexed prostate-specific antigen. *Biosens. Bioelectron.* **145**, 111719 (2019).
109. Niedbala, R. S. et al. Detection of analytes by immunoassay using up-converting phosphor technology. *Anal. Biochem.* **293**, 22–30 (2001).
110. Corstjens, P. et al. Use of up-converting phosphor reporters in lateral-flow assays to detect specific nucleic acid sequences: a rapid, sensitive DNA test to identify human papillomavirus type 16 infection. *Clin. Chem.* **47**, 1885–1893 (2001).
111. Hampl, J. et al. Upconverting phosphor reporters in immunochromatographic assays. *Anal. Biochem.* **288**, 176–187 (2001).
112. Kim, J. et al. Rapid and background-free detection of avian influenza virus in opaque sample using NIR-to-NIR upconversion nanoparticle-based lateral flow immunoassay platform. *Biosens. Bioelectron.* **112**, 209–215 (2018).
113. He, H. et al. Quantitative lateral flow strip sensor using highly doped upconversion nanoparticles. *Anal. Chem.* **90**, 12356–12360 (2018).
114. You, M. et al. Household fluorescent lateral flow strip platform for sensitive and quantitative prognosis of heart failure using dual-color upconversion nanoparticles. *ACS Nano* **11**, 6261–6270 (2017).
115. Gong, Y. et al. A portable and universal upconversion nanoparticle-based lateral flow assay platform for point-of-care testing. *Talanta* **201**, 126–133 (2019).
116. Khreich, N. et al. Detection of *Staphylococcus* enterotoxin B using fluorescent immunoliposomes as label for immunochromatographic testing. *Anal. Biochem.* **377**, 182–188 (2008).
117. Baeumner, A. J., Jones, C. & Yee, C. A generic sandwich-type biosensor with nanomolar detection limits. *Anal. Bioanal. Chem.* **378**, 1587–1593 (2004).
118. Edwards, K. A. & Baeumner, A. J. Optimization of DNA-tagged dye-encapsulating liposomes for lateral-flow assays based on sandwich hybridization. *Anal. Bioanal. Chem.* **386**, 1335–1343 (2006).
119. Edwards, K. A., Korff, R. & Baeumner, A. J. Liposome-enhanced lateral-flow assays for clinical analyses. *Methods Mol. Biol.* **1571**, 407–434 (2017).
120. Urusov, A. E., Zherdev, A. V. & Dzantiev, B. B. Towards lateral flow quantitative assays: detection approaches. *Biosensors* **9**, 89 (2019).
121. Yang, J. et al. Detection platforms for point-of-care testing based on colorimetric, luminescent and magnetic assays: a review. *Talanta* **202**, 96–110 (2019).
122. Nash, M. A., Waitumbi, J. N., Hoffman, A. S., Yager, P. & Stayton, P. S. Multiplexed enrichment and detection of malarial biomarkers using a stimuli-responsive iron oxide and gold nanoparticle reagent system. *ACS Nano* **6**, 6776–6785 (2012).
123. Marquina, C. et al. GMR sensors and magnetic nanoparticles for immuno-chromatographic assays. *J. Magn. Magn. Mater.* **324**, 3495–3498 (2012).
124. Ryu, Y., Jin, Z., Kang, M. S. & Kim, H. S. Increase in the detection sensitivity of a lateral flow assay for a cardiac marker by oriented immobilization of antibody. *Biochip J.* **5**, 193–198 (2011).
125. Wang, D. B. et al. Detection of *Bacillus anthracis* spores by superparamagnetic lateral-flow immunoassays based on 'Road Closure'. *Biosens. Bioelectron.* **67**, 608–614 (2015).
126. Liu, D. et al. A modified lateral flow immunoassay for the detection of trace aflatoxin M1 based on immunomagnetic nanobeads with different antibody concentrations. *Food Control* **51**, 218–224 (2015).
127. Zheng, C., Wang, X., Lu, Y. & Liu, Y. Rapid detection of fish major allergen parvalbumin using superparamagnetic nanoparticle-based lateral flow immunoassay. *Food Control* **26**, 446–452 (2012).
128. Panferov, V. G., Safenkova, I. V., Zherdev, A. V. & Dzantiev, B. B. Setting up the cut-off level of a sensitive barcode lateral flow assay with magnetic nanoparticles. *Talanta* **164**, 69–76 (2017).
129. Lago-Cachon, D. et al. Scanning magneto-inductive sensor for quantitative assay of prostate-specific antigen. *IEEE Magn. Lett* **8**, 1–5 (2017).
130. Moyano, A. et al. Magnetic immunochromatographic test for histamine detection in wine. *Anal. Bioanal. Chem.* **411**, 6615–6624 (2019).
131. Qin, Z. et al. Significantly improved analytical sensitivity of lateral flow immunoassays by using thermal contrast. *Angew. Chem. Int. Ed. Engl.* **51**, 4358–4361 (2012).
132. Wang, Y. et al. Thermal contrast amplification reader yielding 8-fold analytical improvement for disease detection with lateral flow assays. *Anal. Chem.* **88**, 11774–11782 (2016).
133. Sinawang, P. D., Rai, V., Ionescu, R. E. & Marks, R. S. Electrochemical lateral flow immunosensor for detection and quantification of dengue NS1 protein. *Biosens. Bioelectron.* **77**, 400–408 (2016).
134. Aller Pellitero, M., Kitsara, M., Eibensteiner, F. & del Campo, F. J. Rapid prototyping of electrochemical lateral flow devices: stencilled electrodes. *Analyst* **141**, 2515–2522 (2016).
135. Ruiz-Vega, G., Kitsara, M., Pellitero, M. A., Baldrich, E. & del Campo, F. J. Electrochemical lateral flow devices: towards rapid immunomagnetic assays. *ChemElectroChem* **4**, 880–889 (2017).
136. Zhu, X., Shah, P., Stoff, S., Liu, H. & Li, C. A paper electrode integrated lateral flow immunosensor for quantitative analysis of oxidative stress induced DNA damage. *Analyst* **139**, 2850–2857 (2014).
137. Cinti, S., Moscone, D. & Arduini, F. Preparation of paper-based devices for reagentless electrochemical (bio)sensor strips. *Nat. Protoc.* **14**, 2437–2451 (2019).

138. Gonzalez-Macia, L., Morrin, A., Smyth, M. R. & Killard, A. J. Advanced printing and deposition methodologies for the fabrication of biosensors and biodevices. *Analyst* **135**, 845 (2010).
139. Li, Z. et al. Pen-on-paper strategy for point-of-care testing: rapid prototyping of fully written microfluidic biosensor. *Biosens. Bioelectron.* **98**, 478–485 (2017).
140. Millipore Sigma. IVD lateral flow: sample, conjugate and absorbent pad basics. https://www.sigmaaldrich.com/technical-documents/articles/ivd-immunoassay/lateral-flow/pads-chemistries-selections-specifications-and-conjugates.html (2020; accessed 28 July 2020).
141. Quesada-González, D. et al. Iridium oxide (IV) nanoparticle-based electrocatalytic detection of PBDE. *Biosens. Bioelectron.* **127**, 150–154 (2019).
142. Parolo, C., Medina-Sánchez, M., de la Escosura-Muñiz, A. & Merkoçi, A. Simple paper architecture modifications lead to enhanced sensitivity in nanoparticle based lateral flow immunoassays. *Lab Chip* **13**, 386–390 (2013).
143. Tsai, T.-T. et al. Development a stacking pad design for enhancing the sensitivity of lateral flow immunoassay. *Sci. Rep* **8**, 17319 (2018).
144. Shao, X.-Y. et al. Rapid and sensitive lateral flow immunoassay method for procalcitonin (PCT) based on time-resolved immunochromatography. *Sensors* **17**, 480 (2017).
145. Li, J., McMillan, D. & Macdonal, J. Enhancing the signal of lateral flow immunoassays by using different developing methods. *Sensors Mater.* **27**, 549–561 (2015).
146. West, M., Walters, F., Phillips, S. & Rowles, D. Enhanced performance of a lateral flow assay: use of a novel conjugate blocking technology to improve performance of a gold nanoparticle-based lateral flow assy (BBI Morffi Whitepaper). https://www.bbisolutions.com/pub/media/wysiwyg/technical_support/BBI_WHITEPAPER_A4_MORFFI_DIGITAL-linked.pdf (2020; accessed 28 July 2020).
147. Phillips, S. Reagent chemistries and labels of choice for lateral flow. https://www.emdmillipore.com/INTERSHOP/static/WFS/Merck-Site/-/Merck/en_US/Freestyle/DIV-Divisional/Events/pdfs/lateral-flow-presentations/reagent-chemistries-and-labels-of-choice-for-lateral-flow.pdf (2020; accessed 28 July 2020).
148. Shim, W.-B., Kim, J.-S., Kim, M.-G. & Chung, D.-H. Rapid and sensitive immunochromatographic strip for on-site detection of sulfamethazine in meats and eggs. *J. Food Sci.* **78**, M1575–M1581 (2013).
149. Yahaya, M. L., Zakaria, N. D., Noordin, R. & Razak, K. A. The effect of nitrocellulose membrane pore size of lateral flow immunoassay on sensitivity for detection of *Shigella* sp. in milk sample. *Mater. Today Proc.* **17**, 878–883 (2019).
150. Sartorius Stedim Biotech. UniSart nitrocellulose membranes: the substrate of choice for protein assays. https://www.sartorius.com/resource/blob/89574/dc103586e857d533c5901961867f5ed9/broch-unisart-nitro-sl-1536-e-1-data.pdf (2018; accessed 28 July 2020).
151. Tovey, E. R. & Baldo, B. A. Protein binding to nitrocellulose, nylon and PVDF membranes in immunoassays and electroblotting. *J. Biochem. Biophys. Methods* **19**, 169–183 (1989).
152. Asiaei, S., Bidgoli, M. R., ZadehKafi, A., Saderi, N. & Siavashi, M. Sensitivity and colour intensity enhancement in lateral flow immunoassay tests by adjustment of test line position. *Clin. Chim. Acta* **487**, 210–215 (2018).
153. Ragavendar, M. S. & Anmol, C. M. A mathematical model to predict the optimal test line location and sample volume for lateral flow immunoassays. *2012 Annual International Conference of the IEEE Engineering in Medicine and Biology Society* 2408–2411 (IEEE, 2012).
154. Fusion 5. Cytiva. https://www.gelifesciences.com/en/us/shop/whatman-laboratory-filtration/whatman-dx-components/lateral-flow-pads/fusion-5-p-00787 (2020; accessed 28 July 2020).
155. Carrell, C. S. et al. Rotary manifold for automating a paper-based *Salmonella* immunoassay. *RSC Adv.* **9**, 29078–29086 (2019).
156. Yang, J. J., Oh, H.-B. & Hwang, S.-H. Paper-based speedy separation of amplified DNA (PASS-DNA): potential for molecular point-of-care testing. *Sens. Actuators B Chem.* **286**, 101–103 (2019).
157. Tang, R. et al. A fully disposable and integrated paper-based device for nucleic acid extraction, amplification and detection. *Lab Chip* **17**, 1270–1279 (2017).
158. Nurul Najian, A. B., Engku Nur Syafirah, E. A. R., Ismail, N., Mohamed, M. & Yean, C. Y. Development of multiplex loop mediated isothermal amplification (m-LAMP) label-based gold nanoparticles lateral flow dipstick biosensor for detection of pathogenic *Leptospira*. *Anal. Chim. Acta* **903**, 142–148 (2016).
159. Chua, A., Yean, C. Y., Ravichandran, M., Lim, B. & Lalitha, P. A rapid DNA biosensor for the molecular diagnosis of infectious disease. *Biosens. Bioelectron.* **26**, 3825–3831 (2011).
160. Choi, D. H. et al. A dual gold nanoparticle conjugate-based lateral flow assay (LFA) method for the analysis of troponin I. *Biosens. Bioelectron.* **25**, 1999–2002 (2010).
161. Hagström, A. E. V. et al. Sensitive detection of norovirus using phage nanoparticle reporters in lateral-flow assay. *PLoS ONE* **10**, e0126571 (2015).
162. Kim, J. et al. Orientational binding modes of reporters in a viral-nanoparticle lateral flow assay. *Analyst* **142**, 55–64 (2017).
163. Zhou, G., Mao, X. & Juncker, D. Immunochromatographic assay on thread. *Anal. Chem.* **84**, 7736–7743 (2012).
164. Meng, L.-L., Song, T.-T. & Mao, X. Novel immunochromatographic assay on cotton thread based on carbon nanotubes reporter probe. *Talanta* **167**, 379–384 (2017).
165. Jia, X., Song, T., Liu, Y., Meng, L. & Mao, X. An immunochromatographic assay for carcinoembryonic antigen on cotton thread using a composite of carbon nanotubes and gold nanoparticles as reporters. *Anal. Chim. Acta* **969**, 57–62 (2017).
166. Seth, M., Mdetele, D. & Buza, J. Immunochromatographic thread-based test platform for diagnosis of infectious diseases. *Microfluid. Nanofluidics* **22**, 45 (2018).
167. Lappalainen, T., Teerinen, T., Vento, P., Hakalahti, L. & Erho, T. Cellulose as a novel substrate for lateral flow assay. *Nord. Pulp Pap. Res. J.* **25**, 536–550 (2010).
168. Du, S., Lin, H., Sui, J., Wang, X. & Cao, L. Nano-gold capillary immunochromatographic assay for parvalbumin. *Anal. Bioanal. Chem.* **406**, 6637–6646 (2014).
169. Qu, X. et al. Development of a nano-gold capillary immunochromatographic assay for rapid and semi-quantitative detection of clenbuterol residues. *Food Anal. Methods* **9**, 2531–2540 (2016).
170. Cao, E., Chen, Y., Cui, Z. & Foster, P. R. Effect of freezing and thawing rates on denaturation of proteins in aqueous solutions. *Biotechnol. Bioeng.* **82**, 684–690 (2003).
171. O'Farrell, B. Lateral flow technology for field-based applications—basics and advanced developments. *Top. Companion Anim. Med.* **30**, 139–147 (2015).
172. Tian, T. et al. Distance-based microfluidic quantitative detection methods for point-of-care testing. *Lab Chip* **16**, 1139–1151 (2016).
173. Leung, W. et al. InfectCheck CRP barcode-style lateral flow assay for semi-quantitative detection of C-reactive protein in distinguishing between bacterial and viral infections. *J. Immunol. Methods* **336**, 30–36 (2008).
174. Mak, W. C., Beni, V. & Turner, A. P. F. Lateral-flow technology: from visual to instrumental. *Trends Analyt. Chem.* **79**, 297–305 (2016).

175. Shah, K. G., Singh, V., Kauffman, P. C., Abe, K. & Yager, P. Mobile phone ratiometric imaging enables highly sensitive fluorescence lateral flow immunoassays without external optical filters. *Anal. Chem.* **90**, 6967–6974 (2018).
176. Zangheri, M. et al. A simple and compact smartphone accessory for quantitative chemiluminescence-based lateral flow immunoassay for salivary cortisol detection. *Biosens. Bioelectron.* **64**, 63–68 (2015).
177. Roda, A. et al. Smartphone-based biosensors: a critical review and perspectives. *Trends Anal. Chem.* **79**, 317–325 (2016).
178. Jiang, N. et al. Lateral and vertical flow assays for point-of-care diagnostics. *Adv. Healthc. Mater.* **8**, e1900244 (2019).
179. de Puig, H., Bosch, I., Gehrke, L. & Hamad-Schifferli, K. Challenges of the nano-bio interface in lateral flow and dipstick immunoassays. *Trends Biotechnol.* **35**, 1169–1180 (2017).
180. Oh, Y. K., Joung, H.-A., Han, H. S., Suk, H.-J. & Kim, M.-G. A three-line lateral flow assay strip for the measurement of C-reactive protein covering a broad physiological concentration range in human sera. *Biosens. Bioelectron.* **61**, 285–289 (2014).
181. Li, J. & Macdonald, J. Multiplexed lateral flow biosensors: technological advances for radically improving point-of-care diagnoses. *Biosens. Bioelectron.* **83**, 177–192 (2016).
182. Gao, Z. et al. Platinum-decorated gold nanoparticles with dual functionalities for ultrasensitive colorimetric in vitro diagnostics. *Nano Lett.* **17**, 5572–5579 (2017).
183. Kim, H., Chung, D.-R. & Kang, M. A new point-of-care test for the diagnosis of infectious diseases based on multiplex lateral flow immunoassays. *Analyst* **144**, 2460–2466 (2019).
184. Mohd Hanafiah, K. et al. Development of multiplexed infectious disease lateral flow assays: challenges and opportunities. *Diagnostics* **7**, 51 (2017).
185. Qin, Q. et al. Algorithms for immunochromatographic assay: review and impact on future application. *Analyst* **144**, 5659–5676 (2019).
186. Liu, Z. et al. An improved detection limit and working range of lateral flow assays based on a mathematical model. *Analyst* **143**, 2775–2783 (2018).
187. Gantelius, J., Bass, T., Sjöberg, R., Nilsson, P. & Andersson-Svahn, H. A lateral flow protein microarray for rapid and sensitive antibody assays. *Int. J. Mol. Sci.* **12**, 7748–7759 (2011).
188. Choi, J. R. et al. An integrated lateral flow assay for effective DNA amplification and detection at the point of care. *Analyst* **141**, 2930–2939 (2016).
189. Jauset-Rubio, M. et al. Ultrasensitive, rapid and inexpensive detection of DNA using paper based lateral flow assay. *Sci. Rep.* **6**, 37732 (2016).
190. Deng, X. et al. Applying strand displacement amplification to quantum dots-based fluorescent lateral flow assay strips for HIV-DNA detection. *Biosens. Bioelectron.* **105**, 211–217 (2018).
191. Ivanov, A. V., Safenkova, I. V., Zherdev, A. V. & Dzantiev, B. B. Nucleic acid lateral flow assay with recombinase polymerase amplification: solutions for highly sensitive detection of RNA virus. *Talanta* **210**, 120616 (2020).
192. Lafleur, L. K. et al. A rapid, instrument-free, sample-to-result nucleic acid amplification test. *Lab Chip* **16**, 3777–3787 (2016).
193. Xu, Y. et al. Nucleic acid biosensor synthesis of an all-in-one universal blocking linker recombinase polymerase amplification with a peptide nucleic acid-based lateral flow device for ultrasensitive detection of food pathogens. *Anal. Chem.* **90**, 708–715 (2018).
194. Cheng, N. et al. Specific and relative detection of urinary microRNA signatures in bladder cancer for point-of-care diagnostics. *Chem. Commun.* **53**, 4222–4225 (2017).
195. Tang, R. et al. Improved sensitivity of lateral flow assay using paper-based sample concentration technique. *Talanta* **152**, 269–276 (2016).
196. Quesada-González, D. et al. Signal enhancement on gold nanoparticle-based lateral flow tests using cellulose nanofibers. *Biosens. Bioelectron.* **141**, 111407 (2019).
197. Bai, Y. et al. A sensitive lateral flow test strip based on silica nanoparticle/CdTe quantum dot composite reporter probes. *RSC Adv.* **2**, 1778 (2012).
198. Zhao, P. et al. Upconversion fluorescent strip sensor for rapid determination of *Vibrio anguillarum*. *Nanoscale* **6**, 3804–3809 (2014).
199. Ambrosi, A., Airò, F. & Merkoçi, A. Enhanced gold nanoparticle based ELISA for a breast cancer biomarker. *Anal. Chem.* **82**, 1151–1156 (2010).
200. Ford, J. Plasma separation: why do you need it and how do you achieve it. DCN Diagnostics. https://dcndx.com/plasma-separation-why-you-need-it/ (2019; accessed 28 July 2020).
201. Nawattanapaiboon, K. et al. Hemoculture and direct sputum detection of mecA-mediated methicillin-resistant *Staphylococcus aureus* by loop-mediated isothermal amplification in combination with a lateral-flow dipstick. *J. Clin. Lab. Anal.* **30**, 760–767 (2016).
202. Xu, S. et al. Lateral flow immunoassay based on polydopamine-coated gold nanoparticles for the sensitive detection of zearalenone in maize. *ACS Appl. Mater. Interfaces* **11**, 31283–31290 (2019).
203. Anfossi, L. et al. A lateral flow immunoassay for the rapid detection of ochratoxin A in wine and grape must. *J. Agric. Food Chem.* **60**, 11491–11497 (2012).
204. Chen, A. & Yang, S. Replacing antibodies with aptamers in lateral flow immunoassay. *Biosens. Bioelectron.* **71**, 230–242 (2015).
205. Rey, E. G., O'Dell, D., Mehta, S. & Erickson, D. Mitigating the hook effect in lateral flow sandwich immunoassays using real-time reaction kinetics. *Anal. Chem.* **89**, 5095–5100 (2017).
206. Wiederhold, N. P. et al. Interlaboratory and interstudy reproducibility of a novel lateral-flow device and influence of antifungal therapy on detection of invasive pulmonary aspergillosis. *J. Clin. Microbiol.* **51**, 459–465 (2013).
207. Christau, S., Moeller, T., Genzer, J., Koehler, R. & von Klitzing, R. Salt-induced aggregation of negatively charged gold nanoparticles confined in a polymer brush matrix. *Macromolecules* **50**, 7333–7343 (2017).
208. Ruiz-Sanchez, A. J. et al. Tuneable plasmonic gold dendrimer nanochains for sensitive disease detection. *J. Mater. Chem. B* **5**, 7262–7266 (2017).
209. Findlay, J. W. A. & Dillard, R. F. Appropriate calibration curve fitting in ligand binding assays. *AAPS J.* **9**, E260–E267 (2007).
210. Holstein, C. A., Griffin, M., Hong, J. & Sampson, P. D. Statistical method for determining and comparing limits of detection of bioassays. *Anal. Chem.* **87**, 9795–9801 (2015).
211. Faber, N. M. The limit of detection is not the analyte level for deciding between "detected" and "not detected". *Accred. Qual. Assur.* **13**, 277–278 (2008).
212. Armbruster, D. A. & Pry, T. Limit of blank, limit of detection and limit of quantitation. *Clin. Biochem. Rev.* **29**(Suppl 1), S49–S52 (2008).
213. Wen, H. W., Borejsza-Wysocki, W., Decory, T. R. & Durst, R. A. Development of a competitive liposome-based lateral flow assay for the rapid detection of the allergenic peanut protein Ara h1. *Anal. Bioanal. Chem.* **382**, 1217–1226 (2005).
214. Apilux, A., Rengpipat, S., Suwanjang, W. & Chailapakul, O. Development of competitive lateral flow immunoassay coupled with silver enhancement for simple and sensitive salivary cortisol detection. *EXCLI J.* **17**, 1198–1209 (2018).
215. Posthuma-Trumpie, G. A., Korf, J. & van Amerongen, A. Development of a competitive lateral flow immunoassay for progesterone: influence of coating conjugates and buffer components. *Anal. Bioanal. Chem.* **392**, 1215–1223 (2008).

216. Corstjens, P. L. A. M. et al. A user-friendly, highly sensitive assay to detect the IFN-γ secretion by T cells. *Clin. Biochem.* **41**, 440–444 (2008).
217. Rivas, L., Medina-Sánchez, M., de la Escosura-Muñiz, A. & Merkoçi, A. Improving sensitivity of gold nanoparticle-based lateral flow assays by using wax-printed pillars as delay barriers of microfluidics. *Lab Chip* **14**, 4406–4414 (2014).

Acknowledgements

We acknowledge the MICROB-PREDICT project that has received funding from the European Union's Horizon 2020 research and innovation programme under grant agreement No. 825694. Financial support from the EU Graphene Flagship Core 2 Project (No. 785219) is also acknowledged. This article reflects only the author's view, and the European Commission is not responsible for any use that may be made of the information it contains. ICN2 is funded by the CERCA programme/Generalitat de Catalunya. The ICN2 is supported by the Severo Ochoa Centres of Excellence programme, funded by the Spanish Research Agency (AEI, grant no. SEV-2017-0706). C. P. acknowledges the Marie Skłodowska-Curie Actions Individual Fellowship; this project has received funding from the European Union's Horizon 2020 research and innovation programme under the Marie Skłodowska-Curie grant agreement No. 795635. E.C. acknowledges Ministerio de Ciencia e Innovación of Spain and Fondo Social Europeo for the Fellowship PRE2018-084856 awarded under the call 'Ayudas para contratos predoctorales para la formación de doctores, Subprograma Estatal de Formación del Programa Estatal de Promoción del Talento y su Empleabilidad en I +D+i', under the framework of 'Plan Estatal de Investigación Científica y Técnica y de Innovación 2017–2020'. E.P.N. acknowledges funding through the EU's Horizon 2020 research and innovation programme under the Marie Skłodowska-Curie grant agreement No. 754510. A.M. acknowledges all previous members of the group who have been contributing in the research done on LFAs.

Author contributions

C.P. and A.S.-T. designed, organized and wrote the whole manuscript, carried out the experiments, analyzed the data and prepared the figures. J.F.B. wrote the sample pad section. E.C. wrote the nanoparticle section. C.F.-C. wrote the type of sample section. L.H. wrote the membrane section and part of the procedure. L.R. wrote the conjugate pad, Fusion 5 and alternative material sections. R.A.-D. wrote the assay evaluation section and prepared the figures. E.P.N. wrote and edited the manuscript. S.C. wrote the future direction and electrochemical readout sections and helped with the conceptualization. D.Q.-C. wrote the cost, patent, production, regulation and approval sections. A.M. supervised the work.

Competing interests

The authors declare no competing interests.

Additional information

Supplementary information is available for this paper at https://doi.org/10.1038/s41596-020-0357-x.

Correspondence and requests for materials should be addressed to A.M.

Peer review information *Nature Protocols* thanks Claudio Baggiani, Daniel T. Kamei and the other, anonymous, reviewer(s) for their contribution to the peer review of this work.

Reprints and permissions information is available at www.nature.com/reprints.

Publisher's note Springer Nature remains neutral with regard to jurisdictional claims in published maps and institutional affiliations.

Received: 29 July 2019; Accepted: 12 May 2020;
Published online: 23 October 2020

Related links

Key references using this protocol:
Parolo, C. et al. *Biosens. Bioelectron.* **40**, 412–416 (2013): https://www.sciencedirect.com/science/article/pii/S0956566312004083
Parolo, C. et al. *Lab Chip* **13**, 386–390 (2013): https://pubs.rsc.org/en/content/articlelanding/2013/LC/C2LC41144J
Rivas, L. et al. *Lab Chip* **14**, 4406–4414 (2014): https://pubs.rsc.org/en/content/articlelanding/2014/LC/C4LC00972J
López-Marzo, A. M. et al. *Biosens. Bioelectron.* **47**, 190–198 (2013): https://www.sciencedirect.com/science/article/pii/S0956566313001292

nature research

Corresponding author(s): Arben Merkoçi

Last updated by author(s): 21/4/20

Reporting Summary

Nature Research wishes to improve the reproducibility of the work that we publish. This form provides structure for consistency and transparency in reporting. For further information on Nature Research policies, see Authors & Referees and the Editorial Policy Checklist.

Statistics

For all statistical analyses, confirm that the following items are present in the figure legend, table legend, main text, or Methods section.

n/a	Confirmed
☐	☒ The exact sample size (*n*) for each experimental group/condition, given as a discrete number and unit of measurement
☐	☒ A statement on whether measurements were taken from distinct samples or whether the same sample was measured repeatedly
☐	☒ The statistical test(s) used AND whether they are one- or two-sided *Only common tests should be described solely by name; describe more complex techniques in the Methods section.*
☒	☐ A description of all covariates tested
☐	☒ A description of any assumptions or corrections, such as tests of normality and adjustment for multiple comparisons
☐	☒ A full description of the statistical parameters including central tendency (e.g. means) or other basic estimates (e.g. regression coefficient) AND variation (e.g. standard deviation) or associated estimates of uncertainty (e.g. confidence intervals)
☒	☐ For null hypothesis testing, the test statistic (e.g. *F*, *t*, *r*) with confidence intervals, effect sizes, degrees of freedom and *P* value noted *Give P values as exact values whenever suitable.*
☒	☐ For Bayesian analysis, information on the choice of priors and Markov chain Monte Carlo settings
☒	☐ For hierarchical and complex designs, identification of the appropriate level for tests and full reporting of outcomes
☒	☐ Estimates of effect sizes (e.g. Cohen's *d*, Pearson's *r*), indicating how they were calculated

Our web collection on statistics for biologists contains articles on many of the points above.

Software and code

Policy information about availability of computer code

Data collection	N/A
Data analysis	Origin 2018 64-bit, ImageJ

For manuscripts utilizing custom algorithms or software that are central to the research but not yet described in published literature, software must be made available to editors/reviewers. We strongly encourage code deposition in a community repository (e.g. GitHub). See the Nature Research guidelines for submitting code & software for further information.

Data

Policy information about availability of data

All manuscripts must include a data availability statement. This statement should provide the following information, where applicable:

- Accession codes, unique identifiers, or web links for publicly available datasets
- A list of figures that have associated raw data
- A description of any restrictions on data availability

The datasets generated during and/or analysed during the current study are available from the corresponding author on reasonable request.

Field-specific reporting

Please select the one below that is the best fit for your research. If you are not sure, read the appropriate sections before making your selection.

☒ Life sciences ☐ Behavioural & social sciences ☐ Ecological, evolutionary & environmental sciences

For a reference copy of the document with all sections, see nature.com/documents/nr-reporting-summary-flat.pdf

Life sciences study design

All studies must disclose on these points even when the disclosure is negative.

Sample size	We tested three sensor per each concentration so to have enough repetition to calculate the standard deviation.
Data exclusions	We have not excluded any data.
Replication	We confirm it.
Randomization	N/A
Blinding	N/A

Reporting for specific materials, systems and methods

We require information from authors about some types of materials, experimental systems and methods used in many studies. Here, indicate whether each material, system or method listed is relevant to your study. If you are not sure if a list item applies to your research, read the appropriate section before selecting a response.

Materials & experimental systems

n/a	Involved in the study
☐	☒ Antibodies
☒	☐ Eukaryotic cell lines
☒	☐ Palaeontology
☒	☐ Animals and other organisms
☒	☐ Human research participants
☒	☐ Clinical data

Methods

n/a	Involved in the study
☒	☐ ChIP-seq
☒	☐ Flow cytometry
☒	☐ MRI-based neuroimaging

Antibodies

Antibodies used	- Capture antibody in test line (Anti-Human IgG (whole molecule) antibody produced in goat, Sigma-Aldrich, Cat. no. I1886) - Detector antibody in conjugate solution (Anti-Human IgG (γ-chain specific) antibody produced in goat, Sigma-Aldrich, Cat. no. B1140) - Capture antibody in control line (Chicken Anti-Goat IgG H&L, Abcam, Cat. No. ab86245) - Target analyte (IgG from human serum, Sigma-Aldrich, Cat. no. I2511)
Validation	We did not carry out any extra validation.